Atmos. Chem. Phys. Discuss., https://doi.org/10.5194/acp-2017-501
Manuscript under review for journal Atmos. Chem. Phys.
Discussion started: 6 June 2017

Effects of model resolution and parameterizations on the simulations of clouds, precipitation, and their interactions with aerosols

Seoung Soo Lee[1], Zhanqing Li[1], Yuwei Zhang[1], Hyelim Yoo[2]

[1]Earth System Science Interdisciplinary Center, University of Maryland, College Park, Maryland

[2]Earth Resources Technology, Inc., National Oceanic and Atmospheric Administration, College Park, Maryland

Corresponding author: Seoung Soo Lee
Office: (303) 497-6615
Cell: (609) 375-6685
Fax: (303) 497-5318
E-mail: cumulss@gmail.com,slee1247@umd.edu

Atmos. Chem. Phys. Discuss., https://doi.org/10.5194/acp-2017-501
Manuscript under review for journal Atmos. Chem. Phys.
Discussion started: 6 June 2017

Abstract

This study investigates the effects of model resolution and microphysics parameterizations on the uncertainties or errors in the simulations of clouds, precipitation, and their interactions with aerosols using the Global Forecast System (GFS) model as one of the representative numerical weather prediction (NWP) models. For this investigation, we used the GFS model results and compare them with those from the cloud-system resolving model (CSRM) simulations as benchmark simulations that adopt high resolutions and full-fledged microphysical processes. These simulations were evaluated against observations and this evaluation demonstrated that the CSRM simulations can function as benchmark simulations. Substantially lower updrafts and associated cloud variables (e.g., cloud mass and condensation) were simulated by the GFS model compared to those simulated by the CSRM. This is mainly due to the coarse resolutions in the GFS model. This indicates that the parameterizations that represent sub-grid processes in the GFS model do not work well and thus need to be improved. Results here also indicate that the use of the coarse resolution in the GFS model lowers the sensitivity of updrafts and cloud variables to increasing aerosol concentrations compared to the CSRM simulations. The parameterization of the saturation process plays an important role in the sensitivity of cloud variables to aerosol concentrations while the parameterization of the sedimentation process has a substantial impact on how cloud variables are distributed vertically. The variation in cloud variables with resolution is much greater and contributes to the discrepancy between the GFS and CSRM simulations to a much greater degree than what happens with varying microphysics parameterizations.

Atmos. Chem. Phys. Discuss., https://doi.org/10.5194/acp-2017-501
Manuscript under review for journal Atmos. Chem. Phys.
Discussion started: 6 June 2017

1. Introduction

The treatment of clouds and precipitation and their interactions with aerosols in the NWP models is likely a major source of errors in the simulations of the water and energy cycles (Sundqvist et al., 1989; Randall et al., 2006; Seifert et al., 2012). The NWP community has recognized that the accurate representation of clouds, precipitation, and cloud-aerosol-precipitation interactions (CAPI) is important for the improvement of the NWP models and thus, some of these models have started to improve the representation by considering CAPI (Morcrette et al., 2011; Sudhakar et al., 2016).

CAPI may not have a substantial impact on the total precipitation amount but they do affect the temporal and spatial variabilities of precipitation (Li et al., 2011; van den Heever et al., 2011; Seifert et al., 2012; Lee and Feingold, 2013; Fan et al., 2013; Lee et al., 2014), whose importance increases as the temporal/spatial scales of forecast decrease. The distribution of extreme precipitation events such as droughts and floods, closely linked to the spatiotemporal variability, has important social and economic implications.

In recent years, resolutions in the NWP models have increased to the point that the traditional cumulus parameterization schemes may no longer work properly. Motivated by this, scale-aware cumulus parameterization schemes (e.g., Bogenschutz and Krueger, 2013; Thayer-Calder et al., 2015; Griffin and Larson, 2016) are being implemented into these models of different resolutions for better representation of clouds and precipitation.

Atmos. Chem. Phys. Discuss., https://doi.org/10.5194/acp-2017-501
Manuscript under review for journal Atmos. Chem. Phys.
Discussion started: 6 June 2017


Atmospheric Chemistry and Physics Discussions

The uncertainties or errors in the simulations of clouds, precipitation, and CAPI in the NWP models may be incurred both from microphysics parameterizations and from model resolutions. The implementation of the cloud microphysics such as the two-moment (e.g. Morrison and Gettelman, 2008; Morrison et al., 2009) and scale-aware schemes are intended to reduce these uncertainties. It is important to first understand and quantify the uncertainties associated with the two-moment scheme and how model resolutions create the uncertainties, as well as the relative significance between the uncertainties associated with the two-moment scheme and those created by the resolutions. These understanding and quantification can provide us with a guideline on how to represent microphysics in the two-moment schemes and sub-grid processes in the scale-aware schemes for the efficient reduction of the uncertainties in the NWP models. Note that the representation of sub-grid processes requires information on the contribution of resolution to the uncertainties and, in this study, we focus on the two-moment scheme developed by Morrison and Gettelman (2008) and Morrison et al. (2009), which is referred to as the MG scheme, henceforth.

Fan et al. (2012) and Khain et al. (2015) have shown that the parameterizations of three key microphysical processes (i.e., saturation, collection, and sedimentation) in microphysical schemes act as a main source of errors in the simulation of clouds, precipitation, and CAPI. We try to identify and quantify the errors or the uncertainties through comparisons between simulations with parameterizations of the three key processes in the MG scheme and the CSRM simulations with full-fledged microphysical processes. Regarding the understanding of the uncertainties arising from the choice of resolution, we also perform comparisons between the high-resolution CSRM simulations and

Atmos. Chem. Phys. Discuss., https://doi.org/10.5194/acp-2017-501
Manuscript under review for journal Atmos. Chem. Phys.
Discussion started: 6 June 2017

the low-resolution simulations, and do additional comparisons with the GFS simulations. This helps gain an understanding of how the microphysical representation and coarse resolution in the GFS model (as compared to those in the CSRM) contribute to the uncertainties in the GFS simulations of clouds and precipitation by accounting for CAPI. Here, the CSRM simulations act as benchmark simulations by representing microphysical processes with high-level sophistication and by resolving cloud-scale physical and dynamic processes with high resolutions.

2. Models

2.1 The CSRM

The Advanced Research Weather Research and Forecasting (ARW) model, a non-hydrostatic compressible model, is the CSRM selected for use in this study. A fifth-order monotonic advection scheme is used for the advection of cloud variables (Wang et al., 2009). The ARW model considers radiation processes by adopting the Rapid Radiation Transfer Model for General Circulation Models (RRTMG) (Fouquart and Bonnel, 1980; Mlawer et al., 1997). The RRTMG considers the effects of aerosols on the effective sizes of hydrometeors and the associated changes in radiation.

For an assessment of the uncertainties in the MG scheme, which is a type of a bulk scheme, we need to use microphysics schemes that are much more sophisticated than the MG scheme. Through extensive comparisons between various types of bin schemes and bulk schemes, Fan et al. (2012) and

Atmos. Chem. Phys. Discuss., https://doi.org/10.5194/acp-2017-501
Manuscript under review for journal Atmos. Chem. Phys.
Discussion started: 6 June 2017

105 Khain et al. (2015) have concluded that the use of bin schemes or bin-bulk schemes is desirable for
106 reasonable simulations of clouds, precipitation, and their interactions with aerosols. This is because
107 these schemes do not use a saturation adjustment, a mass-weight mean terminal velocity, or constant
108 collection efficiencies that have been used in bulk schemes. Instead, bin schemes use predicted
109 supersaturation levels, and terminal velocities and collection efficiencies that vary with the sizes of
110 hydrometeors. Based on the work by Fan et al. (2012) and Khain et al. (2015), this study considers bin
111 schemes to be a full-fledged microphysics schemes against which the uncertainties in the MG scheme
112 can be assessed. Hence, a bin scheme is adopted in the CSRM used here.

113 The bin scheme adopted by the CSRM is based on the Hebrew University Cloud Model described
114 by Khain and Lynn (2009). The bin scheme solves a system of kinetic equations for the size distribution
115 functions of water drops, ice crystals (plate, columnar and branch types), snow aggregates, graupel and
116 hail, as well as cloud condensation nuclei. Each size distribution is represented by 33 mass-doubling
117 bins, i.e., the mass of a particle m_k in the k^{th} bin is $m_k = 2m_{k-1}$.

118 It is assumed that aerosol particles are composed of ammonium sulfate. The aerosol size
119 distribution is calculated prognostically with sinks and sources, which include advection, droplet
120 nucleation, and aerosol regeneration from droplet evaporation (Fan et al., 2009). Aerosol activation is
121 calculated according to the Köhler theory, i.e., aerosol particles with radii exceeding the critical value at
122 a grid point are activated to become droplets based on predicted supersaturation, and the corresponding
123 bins of the aerosol spectra are emptied. After activation, the aerosol mass is transported within
124 hydrometeors by collision-coalescence and removed from the atmosphere once hydrometeors that

Atmos. Chem. Phys. Discuss., https://doi.org/10.5194/acp-2017-501
Manuscript under review for journal Atmos. Chem. Phys.
Discussion started: 6 June 2017

125 contain aerosols reach the surface. Aerosol particles return to the atmosphere upon evaporation or the
126 sublimation of hydrometeors that contain them.
127
128 **2.2 The GFS model**
129
130 The GFS model is a global NWP model that is run by the National Oceanic and Atmospheric
131 Administration (NOAA). The GFS model has 64 vertical sigma-pressure hybrid layers and a T382 (~ 35
132 km) horizontal resolution. Output fields for a forecast generated at 3-hour intervals (i.e. at 03, 06, 09, 12,
133 15, 18, 21, 24 universal coordinated time, or Z), starting from the control time of 00Z, are used for this
134 study.
135 The GFS model posts parameters for 21 vertically different layers. From the surface (1000 hPa) to
136 the 900-hPa level, the vertical resolution is 25 hPa. Less than 900 hPa, there are 16 levels at a 50-hPa
137 resolution up to 100 hPa. The cloud phase is determined by the mean temperature (Tc) of a cloud layer
138 which is defined as the average of temperatures at the top and bottom of a cloud layer. If Tc is less than
139 258.16 K, the cloud layer is an ice cloud; otherwise, it is a water cloud.
140 A prognostic condensate scheme by Moorthi et al. (2001) has been used to parameterize clouds in
141 the GFS model. In this scheme, cloud mass, one of the representative cloud variables, evolves by
142 considering the cloud-mass advection, diffusion and conversion to precipitation, and the diagnosed sub-
143 grid and grid-scale condensation and evaporation. The grid-scale condensation and evaporation are
144 calculated based on Sundqvist et al. (1989) and Zhao and Carr (1997), while the sub-grid condensation

Atmos. Chem. Phys. Discuss., https://doi.org/10.5194/acp-2017-501
Manuscript under review for journal Atmos. Chem. Phys.
Discussion started: 6 June 2017

and evaporation are calculated based on a cumulus parameterization that adopts the mass-flux approach. This cumulus parameterization was developed by Moorthi et al. (2001) based on a simplified Arakawa-Schubert scheme (Pan and Wu, 1995).

3. The cases

3.1 The Seoul case

A mesoscale convective system (MCS) was observed over Seoul, Korea (37.57°N, 126.97°E; 0900 local solar time (LST) 26 July 2011–0900 LST 27 July 2011). This case, referred to as the Seoul case, involved heavy rainfall with a maximum precipitation rate of ~150 mm h^{-1}. This heavy rainfall caused flash floods and landslides on a mountain at the southern flank of the city, leading to the deaths of 60 people.

At 0900 LST July 26th 2011, favorable synoptic-scale features for the development of heavy rainfall over Seoul were observed. The western Pacific subtropical high (WPSH) was located over the southeast of Korea and Japan, and there was a low-pressure trough over north China (Figure 1a). Low-level jets between the flank of the WPSH and the low-pressure system brought warm, moist air from the Yellow Sea to the Korean Peninsula (Figure 1b). Transport of warm and moist air by the southwesterly low-level jet is an important condition for the development of heavy rainfall events over Seoul (Hwang and Lee, 1993; Sun and Lee, 2002).

Atmos. Chem. Phys. Discuss., https://doi.org/10.5194/acp-2017-501
Manuscript under review for journal Atmos. Chem. Phys.
Discussion started: 6 June 2017

165

166 **3.2 The Houston case**

167

168 An MCS was observed over Houston, Texas (29.42°N, 94.45°W; 0700 LST 18 July 2013–0400 LST 19
169 July 2013). The Houston case involved moderate rainfall with a maximum precipitation rate of ~50 mm
170 h^{-1}.

171 At 0500 LST, two hours before the initiation of convection, the low-level wind in and around
172 Houston was southerly (Figure 1c), favoring the transport of water vapor from the Gulf of Mexico to
173 the Houston area. Associated with this, the environmental convective available potential energy (CAPE)
174 (Figure 1d) in and around Houston along the coastline was high (as represented by red areas in Figure
175 1d). The high CAPE provided a favorable condition for the development of the MCS.

176

177 **4. Simulations**

178

179 **4.1 The CSRM simulations**

180

181 Using the ARW model and its bin scheme, a three-dimensional CSRM simulation of the observed MCS
182 was performed over the MCS period for each of the cases.

183 Initial and boundary conditions for the control run are derived from the National Centers for
184 Environmental Prediction GFS final (FNL) analysis. All experiments employ a prognostic surface skin

Atmos. Chem. Phys. Discuss., https://doi.org/10.5194/acp-2017-501
Manuscript under review for journal Atmos. Chem. Phys.
Discussion started: 6 June 2017

temperature scheme (Zeng and Beljaars, 2005) and a revised roughness length formulation (Donelan et al., 2004).

The control run for each of the cases consists of a domain with a Lambert conformal map projection. The domain is marked by the rectangle for the Seoul case in Figure 2a and the domain for the Houston case is shown in Figure 2b. While the control run for the Seoul case is referred to as "the control-Seoul run", the control run for the Houston case is referred to as "the control-Houston run", henceforth. The domain for the Seoul (Houston) case covers the Seoul (Houston) area and to resolve cloud-scale processes, a 500-m horizontal resolution is applied to the domain. The domain has 41 vertical layers with resolutions ranging from 70 m near the surface to 800 m at the model top (~50 hPa). Note that the cumulus parameterization scheme is not used in this domain where convective rainfall generation is assumed to be explicitly resolved. Based on observations, the aerosol concentration at the surface at the first time step is set at 5500 (1500) cm^{-3} for the Seoul (Houston) case. Above the top of the planetary boundary layer (PBL) around 2 km, the aerosol concentration reduces exponentially.

To examine and isolate CAPI, i.e., the effect of increasing the loading of aerosols on clouds and precipitation, the control run is repeated with the aerosol concentration at the first time step reduced by a factor of 10. This factor is based on observations showing that that reduction in aerosol loading between polluted days and clean days is generally tenfold over Seoul and Houston(Lance et al., 2009; Kim et al., 2014). This simulation is referred to as the low-aerosol-Seoul run for the Seoul case and the low-aerosol-Houston run for the Houston case. Since the control-Seoul run and the control-Houston run involve higher aerosol concentrations than the low-aerosol-Seoul run and the low-aerosol-Houston run,

Atmos. Chem. Phys. Discuss., https://doi.org/10.5194/acp-2017-501
Manuscript under review for journal Atmos. Chem. Phys.
Discussion started: 6 June 2017

205 respectively, for naming purposes, the control-Seoul run and the control-Houston run are also
206 referred to as the high-aerosol-Seoul run and the high-aerosol-Houston run, respectively.
207 In addition to the simulations described above, more simulations were performed to fulfill the goals
208 of this study (Table 1). Details of those simulations are given in the following sections.
209
210 **4.2 The GFS simulations**
211
212 Note that the GFS produces the forecast data over the globe and for this study, we use the data
213 only during the MCS period and only at grid points in the domain for each case. We collect GFS data in
214 the domain and then average the data over those grid points at each of the GFS time steps for each of
215 the cases. For the comparison between the GFS and CSRM simulations at specific time steps over the
216 MCS period, these averaged data are compared to the CSRM simulations during the period. In case the
217 time and domain-averaged GFS data are compared to the CSRM counterparts, these averaged data are
218 averaged again over the MCS period and compared to their CSRM counterparts.
219
220 **5. Results**
221
222 **5.1 Test on the effects of resolution on the simulations of clouds,**
223 **precipitation, and CAPI**
224

Atmos. Chem. Phys. Discuss., https://doi.org/10.5194/acp-2017-501
Manuscript under review for journal Atmos. Chem. Phys.
Discussion started: 6 June 2017

225 **5.1.1 Cloud liquid content (CLC) and cloud ice content (CIC)**

226

227 To test the effects of resolution on the simulations of clouds, precipitation, and their interactions with
228 aerosols, we repeat the standard CSRM runs at the 500-m resolution (i.e., the high-aerosol-Seoul run,
229 the low-aerosol-Seoul run, the high-aerosol-Houston run, and the low-aerosol-Houston run) by using
230 15- and 35-km resolutions instead. These resolutions are similar to those generally adopted by current
231 NWP models (e.g., the GFS model) and thus comparisons between these repeated simulations and the
232 CSRM simulations can evaluate how coarse resolutions adopted by the NWP models affect the
233 simulations of clouds, precipitation, and their interactions with aerosols. The repeated simulations at the
234 15-km resolution are referred to as the high-aerosol-15-Seoul run, the low-aerosol-15-Seoul run, the
235 high-aerosol-15-Houston run, and the low-aerosol-15-Houston run, while the repeated simulations at
236 the 35-km resolution are referred to as the high-aerosol-35-Seoul run, the low-aerosol-35-Seoul run, the
237 high-aerosol-35-Houston run, and the low-aerosol-35-Houston run. In this study, simulations whose
238 name includes "high-aerosol" represent the polluted scenario, while those whose name includes "low-
239 aerosol" represent the clean scenario. In the following, we describe results from the standard and
240 repeated simulations. For the Houston case, no clouds form at the 35-km resolution, so the description
241 of results is only done for results at the 15-km resolution.

242 Figures 3a and 3b show the vertical distributions of the time- and domain-averaged CLC in the
243 simulations for the Seoul case and the Houston case, respectively. Figures 4a and 4b show the vertical
244 distributions of the time- and domain-averaged CIC in the simulations for the Seoul case and the

Atmos. Chem. Phys. Discuss., https://doi.org/10.5194/acp-2017-501
Manuscript under review for journal Atmos. Chem. Phys.
Discussion started: 6 June 2017

Houston case, respectively. There are increases in the cloud mass (represented by CLC and CIC) with increasing aerosol concentration between the polluted scenario and the clean scenario not only for both the Seoul and Houston cases but also at all resolutions considered. There are substantial decreases in the cloud mass at the 15- and 35-km resolutions compared to the cloud mass in the simulations at the 500-m resolution. In addition, increases in the cloud mass with increasing aerosol concentration reduce substantially as the resolution coarsens. At the 500-m resolution, on average, there is about a ~30–50% increase in cloud mass, while at the 15- or 35-km resolutions, there is only a ~2–5% increase in cloud mass in both cases.

For both the Seoul and Houston cases, comparisons between the cloud mass produced by the GFS simulations and that produced by the ARW simulations show that the GFS-simulated cloud mass is similar to that in the ARW simulations at the 15- and 35-km resolutions. However, the GFS-simulated cloud mass is much smaller than that in the ARW simulations at the 500-m resolution, i.e., the CSRM simulations. This suggests that the coarse resolutions used in the GFS simulations are an important cause of the differences in cloud mass between the CSRM simulations and the GFS simulations.

5.1.2 Liquid water path (LWP) and ice water path (IWP)

Figures 5a and 5b show the time series of the domain-averaged LWP and IWP for the Seoul case while Figures 6a and 6b show the same for the Houston case. Note that LWP and IWP are the vertical

Atmos. Chem. Phys. Discuss., https://doi.org/10.5194/acp-2017-501
Manuscript under review for journal Atmos. Chem. Phys.
Discussion started: 6 June 2017

integrals of CLC and CIC, respectively. Consequently, the same behavior as that of CLC and CIC is seen, namely, there are increases in LWP and IWP with increasing aerosol concentrations between the polluted and clean scenarios at all resolutions, while there are decreases in LWP and IWP with the use of the 15- and 35-km resolutions compared to using the 500-m resolution. Also, the sensitivity of LWP and IWP to increasing aerosol concentrations reduces significantly as the resolution coarsens.

In Figures 5 and 6, satellite-observed LWP and IWP for both cases follow reasonably well their CSRM-simulated counterparts for the polluted scenario. This shows that the CSRM simulations perform well and can thus represent benchmark simulations. The GFS-produced LWP and IWP are similar to those in the ARW simulations at the 15- and 35-km resolutions and are much smaller in magnitude than those from the CSRM simulations and observations. Hence, the discrepancy in LWP and IWP between the GFS and CSRM simulations or that between the GFS simulations and observations is closely linked to the coarse resolution adopted by the GFS simulations. Taking the CSRM simulations as benchmark simulations, we see that GFS simulations underestimate the cloud mass compared to observations mainly due to the coarse resolution adopted by the GFS model.

Among the ARW simulations, the sensitivity of the cloud mass to increasing aerosol concentrations reduces considerably with coarsening resolution. CSRM simulations are benchmark simulations so the sensitivity in the CSRM simulations is the benchmark sensitivity. Note that the GFS simulation results and the ARW simulations at coarse resolutions of 15 and 35 km are similar. Their sensitivities are thus also likely similar, i.e., the sensitivity of the cloud mass to increasing aerosol

Atmos. Chem. Phys. Discuss., https://doi.org/10.5194/acp-2017-501
Manuscript under review for journal Atmos. Chem. Phys.
Discussion started: 6 June 2017

284 concentrations in the GFS simulation is likely to be underestimated compared to the benchmark
285 sensitivity of the CSRM simulations.
286
287 **5.1.3 Updrafts, condensation, and deposition**
288
289 To understand the response of the cloud mass to increasing aerosol concentrations, and the variation in
290 the cloud mass and its response to increasing aerosol concentrations with varying resolutions as shown
291 in Figures 3, 4, 5, and 6, we calculate updraft mass fluxes since these fluxes control supersaturation that
292 in turn controls condensation and deposition as key determination factors for the cloud mass. We also
293 obtain condensation and deposition rates. The vertical distributions of time- and domain-averaged
294 updraft mass fluxes, condensation rates, and deposition rates for the Seoul and Houston cases are shown
295 in Figures 7, 8, and 9, respectively.
296 As seen for the cloud mass, updraft mass fluxes, and condensation and deposition rates increase
297 with increasing aerosol concentrations between the polluted scenario and the clean scenario at all
298 resolutions and for all cases considered. Aerosol-induced percentage increases in updraft mass fluxes,
299 and deposition and condensation rates at the 500-m resolution are approximately one order of
300 magnitude greater than those at the 15-km and 35-km resolutions. Stated differently, the sensitivity of
301 updraft mass fluxes to increasing aerosol concentrations reduces substantially with coarsening
302 resolution and due to this, the sensitivity of deposition and condensation rates, and thus the cloud mass,
303 to increasing aerosol concentrations also reduces substantially with coarsening resolution.

Atmos. Chem. Phys. Discuss., https://doi.org/10.5194/acp-2017-501
Manuscript under review for journal Atmos. Chem. Phys.
Discussion started: 6 June 2017

Similar to the situation with the cloud mass, the GFS-produced updraft mass fluxes are much smaller than those produced by the ARW simulations at the 500-m resolution (or the CSRM simulations) and similar to those produced by the ARW simulations at the 15- and 35-km resolutions (Figure 7). Hence, the discrepancy in updraft mass fluxes between the GFS simulations and the CSRM simulations is closely linked to the discrepancy in resolutions between these two types of simulations. The underestimation of the updraft mass fluxes in the GFS simulations is mainly due to the coarse resolution adopted by the GFS model. Taking the sensitivity of updraft mass fluxes to increasing aerosol concentrations in the CSRM simulations as the benchmark sensitivity, the GFS simulations likely also underestimate the sensitivity.

Figure 10 shows the frequency distribution of updrafts over the updraft speed, which is normalized over the domain and the simulation period. We first calculate the frequency over the domain at each time step and in each discretized updraft bin. The frequency in each bin and at each time step is then divided by the total number of grid points in the whole domain. The normalized frequency at each time step is summed over all of the time steps in each updraft bin. This sum is divided by the total number of time steps as the final step in the normalization process. With coarsening resolution, the normalized frequency of weak updrafts with speeds less than ~2 m s^{-1} increases for both scenarios in both cases. However, the normalized frequency of strong updrafts with speeds greater than ~2 m s^{-1} reduces with coarsening resolution. The frequency shift from high-level updraft speeds to low-level speeds leads to a reduction in mean updrafts with coarsening resolution for both scenarios in both cases.

Atmos. Chem. Phys. Discuss., https://doi.org/10.5194/acp-2017-501
Manuscript under review for journal Atmos. Chem. Phys.
Discussion started: 6 June 2017

The updraft frequency is greater in the polluted scenario than in the clean scenario at all resolutions and for all cases. The overall difference in the frequency between the scenarios reduces with coarsening resolution. This is associated with the reduction in the sensitivity of the averaged updrafts to increasing aerosol concentrations with coarsening resolution. In particular, the difference in the frequency for weak updrafts (speeds less than ~2 m s^{-1}) between the scenarios does not vary much with coarsening resolution. On average, the percentage difference for weak updrafts is less than 2–3% at all resolutions. However, the difference for strong updrafts varies significantly with varying resolution. The mean difference for strong updrafts varies from ~30–60% for the 500-m resolution to less than ~5–6 % for the 15- and 35-km resolutions. Numerous studies (e.g., Khain et al., 2005; Seifert and Beheng, 2006; Tao et al., 2007, 2012; van den Heever and Cotton, 2007; Storer et al., 2010; Lee et al., 2013, 2017) have shown that aerosol-induced invigoration of convection through aerosol-induced increases in freezing or aerosol-induced intensification of gust fronts is the main mechanism behind aerosol-induced increases in updraft mass fluxes or the intensity of updrafts. Based on this, analyses of the updraft frequency here suggest that strong updrafts are more sensitive to aerosol-induced invigoration than weak updrafts. The variation in the sensitivity of the averaged updrafts to increasing aerosol concentrations at varying resolutions is associated more with the variation of the response of strong updrafts to aerosol-induced invigoration at varying resolutions than with that of weak updrafts. Another point to make here is that the frequency of weak updrafts is overestimated while that of strong updrafts is underestimated at coarse resolutions compared to the frequencies in the fine-resolution CSRM simulations.

Atmos. Chem. Phys. Discuss., https://doi.org/10.5194/acp-2017-501
Manuscript under review for journal Atmos. Chem. Phys.
Discussion started: 6 June 2017

343

344 **5.1.4 Evaporation and precipitation distributions**

345

346 Aerosol-induced increases in evaporation and associated cooling affect downdrafts, and changes in
347 downdrafts in turn affect gust fronts. Aerosol-induced changes in the intensity of gust fronts affect the
348 organization of cloud systems, which is characterized by cloud-cell spatiotemporal distributions. In
349 general, aerosol-induced greater increases in evaporation result in aerosol-induced greater changes in
350 the intensity of gust fronts and in cloud system organization (Tao et al., 2007, 2012; van den Heever
351 and Cotton, 2007; Storer et al., 2010; Lee et al., 2013, 2017).

352 Considering that individual cloud cells act as individual sources of precipitation, aerosol-induced
353 changes in the cloud system organization can alter precipitation spatiotemporal distributions, which
354 play an important role in hydrological circulations. It is thus important to examine how the response of
355 evaporation to increasing aerosol concentrations varies with varying resolution, i.e., to see how coarse
356 resolutions affect the quality of simulations of aerosol effects on hydrological circulations. Motivated
357 by this, evaporation rates are obtained and are shown in Figure 11.

358 As seen in the above-described variables, evaporation rates increase as the aerosol concentration
359 increases and the sensitivity of the evaporation rate to increasing aerosol concentrations reduces with
360 coarsening resolution among the ARW simulations. This suggests that the sensitivities of the cloud
361 system organization and precipitation distributions to increasing aerosol concentrations likely also
362 reduce with coarsening resolution, as reported in previous studies (e.g., Tao et al., 2007, 2012; van den

Atmos. Chem. Phys. Discuss., https://doi.org/10.5194/acp-2017-501
Manuscript under review for journal Atmos. Chem. Phys.
Discussion started: 6 June 2017

Heever and Cotton, 2007; Storer et al., 2010; Lee et al., 2013, 2017). This is confirmed by the distribution of normalized precipitation frequency over precipitation rates shown in Figure 12. Similar to the normalization for the updraft frequency, we first calculate the frequency of surface precipitation rates at each time step and in each discretized precipitation rate bin. The frequency in each bin and at each time step is then divided by the total number of grid points at the surface. The normalized frequency at each time step is summed over all of the time steps. This sum is divided by the total number of time steps as the final step in the normalization process. Figure 12 shows that due to the reduction in the sensitivity of evaporative cooling to increasing the aerosol concentration as the resolution coarsens, differences in the distribution of precipitation frequency between the polluted scenario and the clean scenario reduce substantially as the resolution coarsens. Taking the 500-m resolution CSRM simulations as benchmark simulations, this suggests that the coarse-resolution GFS simulations likely underestimate the sensitivity of evaporative cooling, cloud system organization, and precipitation distributions to increasing aerosol concentrations.

5.2 Test on the effects of microphysics parameterizations on the simulations of clouds, precipitation, and CAPI

As mentioned previously, among microphysical processes, saturation, sedimentation, and collection processes are those whose parameterizations are a main cause of errors in the simulation of clouds, precipitation, and CAPI. Motivated by this, we focus on these three microphysical processes for testing

Atmos. Chem. Phys. Discuss., https://doi.org/10.5194/acp-2017-501
Manuscript under review for journal Atmos. Chem. Phys.
Discussion started: 6 June 2017

383 the effects of microphysics parameterizations on the simulations of clouds, precipitation, and CAPI.
384 As a preliminary step to this test, we first focus on the effects of microphysics parameterizations on the
385 simulation of the cloud mass, which plays a key role in cloud radiative properties and precipitation.
386 Based on Figures 3 and 4, we focus on the CLC, which accounts for the bulk of the total cloud mass.

387 Figure 13 shows the vertical distributions of the time- and domain-averaged CLC. In Figure 13a,
388 solid red and black lines represent the high-aerosol-Seoul run and the low-aerosol-Seoul run,
389 respectively, while in Figure 13b, those lines represent the high-aerosol-Houston run and the low-
390 aerosol-Houston run, respectively. Note that these runs shown in the figure are performed using the bin
391 scheme and the 500-m resolution. These simulations were repeated with the Morrison two-moment
392 scheme. These repeated simulations using the MG scheme, referred to as the high-aerosol-MG-Seoul
393 run, the low-aerosol-MG-Seoul run, the high-aerosol-MG-Houston run and the low-aerosol-MG-
394 Houston run, are represented by solid yellow and green lines in Figure 13. Between the high-aerosol
395 and low-aerosol runs using the MG scheme for the two cases, there is an increase in CLC with
396 increasing aerosol concentration. However, this increase is much smaller than that between the high-
397 aerosol and low-aerosol runs using the bin scheme for the two cases. In addition, there is a significant
398 difference in the shape of the vertical profile of CLC between the simulations with the MG scheme and
399 those with the bin scheme for both cases. Here, the shape is represented by the peak value of CLC and
400 the altitude of the peak value in the vertical profile. The peak value is higher in the simulations with the
401 bin scheme than in the simulations with the MG scheme for each of the polluted and clean scenarios.
402 The altitude of the peak value is lower in the simulations with the bin scheme than in the simulations

Atmos. Chem. Phys. Discuss., https://doi.org/10.5194/acp-2017-501
Manuscript under review for journal Atmos. Chem. Phys.
Discussion started: 6 June 2017

403 with the MG scheme. For the Seoul (Houston) case, the altitude is ~2 (3) km in the simulations with
404 the bin scheme, while it is ~5 km in those with the MG scheme.

405 We next test how the parameterization of saturation processes affects the simulations by
406 comparing the supersaturation prediction in the bin scheme to the saturation adjustment in the MG
407 scheme. To do this, the simulations with the bin scheme are repeated after replacing the supersaturation
408 prediction in the bin scheme with the saturation adjustment in the MG scheme. These repeated
409 simulations are referred to as the high-aerosol-sat-Seoul run, the low-aerosol-sat-Seoul run, the high-
410 aerosol-sat-Houston run, and the low-aerosol-sat-Houston run. The high-aerosol-sat-Seoul run and the
411 low-aerosol-sat-Seoul run for the Seoul case and the high-aerosol-sat-Houston run and the low-aerosol-
412 sat-Houston run for the Houston case are represented by dashed lines in Figure 13. As in the other
413 simulations, there is an increase in CLC with increasing aerosol concentrations between the high-
414 aerosol-sat and the low-aerosol-sat runs for the two cases. However, this increase is much smaller than
415 that between the high-aerosol and low-aerosol runs for the two cases, but is similar to that between the
416 high-aerosol-MG and low-aerosol-MG runs for the two cases. This suggests that the sensitivity of the
417 CLC to increasing aerosol concentrations is affected by the parameterization of the saturation process
418 and that the use of the saturation adjustment reduces the sensitivity compared to using the
419 supersaturation prediction.

420 The high-aerosol-sat-Seoul run, the low-aerosol-sat-Seoul run, the high-aerosol-sat-Houston run,
421 and the low-aerosol-sat-Houston run are repeated by replacing the bin-scheme sedimentation with the
422 sedimentation from the MG scheme as a way of testing the effects of the parameterization of

Atmos. Chem. Phys. Discuss., https://doi.org/10.5194/acp-2017-501
Manuscript under review for journal Atmos. Chem. Phys.
Discussion started: 6 June 2017

sedimentation on the simulations. These repeated runs are referred to as the high-aerosol-sed-Seoul run, the low-aerosol-sed-Seoul run, the high-aerosol-sed-Houston run, and the low-aerosol-sed-Houston run. These runs are identical to the high-aerosol-Seoul run, the low-aerosol-Seoul run, the high-aerosol-Houston run and the low-aerosol-Houston run, respectively, except for the parameterization of the saturation and sedimentation processes. As mentioned previously, terminal velocities vary as hydrometeor sizes vary in the bin scheme, while the MG scheme adopts mass-weight mean terminal velocities for the calculation of the sedimentation process.

The vertical distributions of the CLC in the high-aerosol-sed-Seoul run, the low-aerosol-sed-Seoul run, the high-aerosol-sed-Houston run, and the low-aerosol-sed-Houston run are represented by dashed lines in Figure 14. Comparisons between the pair of high-aerosol-sed and low-aerosol-sed runs for the two cases and the pair of high-aerosol-MG and low-aerosol-MG runs for the two cases show that not only the increases in the CLC with increasing aerosol concentrations but also the shapes of the vertical distribution of the CLC in the high-aerosol-sed and low-aerosol-sed runs for the two cases are similar to those in the high-aerosol-MG and low-aerosol-MG runs for the two cases. This demonstrates that differences in the shape of the vertical profile of CLC between the bin-scheme simulations and the MG-scheme simulations are not explained by differences in the representation of the saturation process alone. This also demonstrates that the representation of the sedimentation process plays an important role in generating the differences in the shape of the vertical profile of CLC.

In Figure 14, we still see differences in the vertical profiles of CLC between the high-aerosol-sed-Seoul and high-aerosol-MG-Seoul runs, and between the low-aerosol-sed-Seoul and low-aerosol-MG-

Atmos. Chem. Phys. Discuss., https://doi.org/10.5194/acp-2017-501
Manuscript under review for journal Atmos. Chem. Phys.
Discussion started: 6 June 2017

Seoul runs, as well as between the high-aerosol-sed-Houston and high-aerosol-MG-Houston runs, and between the low-aerosol-sed-Houston and low-aerosol-MG-Houston runs. To understand the cause of these differences, the high-aerosol-sed-Seoul run, the low-aerosol-sed-Seoul run, the high-aerosol-sed-Houston run, and the low-aerosol-sed-Houston run are repeated again with the MG-scheme collection process. These repeated runs are referred to as the high-aerosol-col-Seoul run, the low-aerosol-col-Seoul run, the high-aerosol-col-Houston run, and the low-aerosol-col-Houston run. These runs are identical to the high-aerosol-Seoul run, the low-aerosol run-Seoul, the high-aerosol-Houston run, and the low-aerosol-Houston run, respectively, except for the parameterization of the saturation, sedimentation, and collection processes. As mentioned previously, collection efficiencies vary as hydrometeor sizes vary in the bin scheme, while the MG scheme uses constant collection efficiencies.

As seen in Figure 15, the remaining differences between the high-aerosol-col-Seoul and high-aerosol-MG-Seoul runs and between the low-aerosol-col-Seoul and low-aerosol-MG-Seoul runs, as well as between the high-aerosol-col-Houston and high-aerosol-MG-Houston runs, and between the low-aerosol-col-Houston and low-aerosol-MG-Houston runs nearly disappear. This demonstrates with fairly good confidence that differences between the high-aerosol-Seoul run (the high-aerosol-Houston run) and the high-aerosol-MG-Seoul run (the high-aerosol-MG-Houston run) or between the low-aerosol-Seoul run (the low-aerosol-Houston run) and the low-aerosol-MG-Seoul run (the low-aerosol-MG-Houston run) are explained by differences in the parameterizations of the saturation, sedimentation, and collection processes between the bin scheme and the MG scheme.

Atmos. Chem. Phys. Discuss., https://doi.org/10.5194/acp-2017-501
Manuscript under review for journal Atmos. Chem. Phys.
Discussion started: 6 June 2017

5.3 Relative importance of resolution and parameterizations

Comparisons between ARW simulations with different resolutions and those with different microphysics parameterizations as shown in Figures 3 and 13 demonstrate that the variation in cloud variables is much greater with respect to the variation in resolution than with the variation in microphysics parameterizations. For example, comparisons between Figures 3 and 13 show that the variation in the time- and domain-averaged cloud mass is ~2–4 times greater as the resolution varies than when the microphysics parameterizations varies. These comparisons also show that the variation in cloud variables with varying resolutions explains the discrepancy between GFS simulations and CSRM simulations and between GFS simulations and observations much better than the variation in microphysics parameterizations. As a first step toward reducing the first-order errors in the GFS simulations, we first need to focus on the reduction in errors that are associated with the use of coarse resolutions in the GFS model.

6. Summary and Discussion

This study examines the uncertainties in the simulations of clouds, precipitation, and CAPI in the NWP models. Here, we focus on those uncertainties that are created by the microphysics parameterizations and by the model resolution chosen. In particular, for the examination of the uncertainties associated

Atmos. Chem. Phys. Discuss., https://doi.org/10.5194/acp-2017-501
Manuscript under review for journal Atmos. Chem. Phys.
Discussion started: 6 June 2017

with microphysics parameterizations, we investigate the contributions of the parameterizations of three key microphysical processes, i.e., saturation, collection, and sedimentation, to the uncertainties.

As a way of examining the uncertainties created by the microphysics parameterizations, we compare the MG scheme (a representative bulk scheme) to the bin scheme, which acts as a benchmark scheme. The vertical distribution of the cloud mass simulated by the MG scheme deviates substantially from that simulated by the bin scheme. In particular, there is a substantial discrepancy in the peak value of the distribution and the altitude of the peak value between the schemes. Also, there is a substantial discrepancy between the schemes in the sensitivity of the cloud mass to increasing aerosol concentrations.

The discrepancy in the sensitivity is closely linked to the discrepancy in the parameterization of the saturation processes between the schemes. The use of the saturation adjustment in the bulk scheme reduces the sensitivity by a factor of ~2 compared to the use of the supersaturation prediction in the bin scheme. The discrepancy in the peak value and its altitude between the schemes is strongly linked to the parameterization of sedimentation in the schemes. The use of identical parameterizations of saturation and sedimentation makes the sensitivity and the peak value and its altitude similar between the schemes, although there still remains a slight difference in the magnitude of the cloud mass. This remaining difference is explained by the discrepancy in the parameterization of the collection process. When the two schemes use identical parameterizations of the saturation, sedimentation, and collection processes, the sensitivity and the peak value and its altitude become nearly identical between the two schemes. This confirms that differences in the parameterizations of the three key processes (i.e., saturation,

Atmos. Chem. Phys. Discuss., https://doi.org/10.5194/acp-2017-501
Manuscript under review for journal Atmos. Chem. Phys.
Discussion started: 6 June 2017

sedimentation, and collection) are the main cause of the differences in the simulations of clouds between the schemes as indicated by Fan et al. (2012) and Khain et al. (2015).

By selecting the simulations with the bin scheme as benchmark simulations, we see that the use of the saturation adjustment, as done in most current NWP models, can lead to an underestimation of the sensitivity of the cloud mass to increasing aerosol concentrations. Fan et al. (2012) and Khain et al. (2015) have also shown that the sensitivity of the cloud mass to increasing aerosol concentrations is lower in the bulk scheme than in the bin scheme. This study shows that the lower sensitivity in the bulk scheme is closely linked to the use of the saturation adjustment in the bulk scheme.

It is well known that the shape of the vertical profile of the cloud mass (i.e., the peak value of the cloud mass and its altitude) or how cloud mass is distributed in the vertical domain has substantial implications for cloud radiative forcing and precipitation processes. This study demonstrates that the different parameterizations of the sedimentation process between the schemes lead to different shapes of the cloud-mass profiles and thus different cloud radiative forcings and precipitation processes. The use of a mass-weight mean terminal velocity for sedimentation as done in the bulk schemes can lead to misleading shapes, cloud radiative forcings, and precipitation processes compared to those in the benchmark bin-scheme simulations where terminal velocities vary as hydrometeor sizes vary.

NWP models (e.g., the GFS model) adopt coarse resolutions. This study shows that the use of coarse resolutions can cause an underestimation of the updraft intensity and thus supersaturation, which leads to an underestimation of the cloud mass. Also, the use of coarse resolutions likely results in the

Atmos. Chem. Phys. Discuss., https://doi.org/10.5194/acp-2017-501
Manuscript under review for journal Atmos. Chem. Phys.
Discussion started: 6 June 2017


Atmospheric Chemistry and Physics Discussions

underestimation of the sensitivity of updrafts and cloud mass and that of evaporation, cloud system organization, and precipitation distributions to increasing aerosol concentrations.

Through the examination of the sensitivity of the results to the resolution chosen, we find that updrafts, associated other cloud variables, and their sensitivity to increasing aerosol concentrations are strongly controlled by small-scale updrafts. When they are resolved with the use of high-resolution models, there are high-level averaged updrafts, associated variables, and their sensitivity but when they are not resolved in low-resolution models, there are low-level averaged updrafts, associated variables, and their sensitivity. This means that small-scale updrafts not resolved with coarse resolutions play an important role in the simulation of the correct magnitude of updrafts, associated variables, and their sensitivity to increasing aerosol concentrations.

The frequency distributions of updrafts simulated in this study show that the frequency of weak updrafts is overestimated while that of strong updrafts is underestimated in the simulations with coarse resolutions compared to those in the CSRM simulations. Hence, the updraft speed shifts toward lower values with coarsening resolution. The difference in the frequency between the polluted and clean scenarios reduces substantially, particularly for strong updrafts, with coarsening resolution. This is why the sensitivity of updrafts and associated cloud variables to increasing aerosol concentrations reduces with coarsening resolution. We see that not resolving small-scale updrafts results in the underestimation of strong updrafts and the overestimation of weak updrafts for both scenarios and in the reduced difference in strong updrafts between the scenarios.

Atmos. Chem. Phys. Discuss., https://doi.org/10.5194/acp-2017-501
Manuscript under review for journal Atmos. Chem. Phys.
Discussion started: 6 June 2017

The GFS simulations use the so-called sub-grid parameterizations (e.g., cumulus parameterizations) that represent sub-grid updrafts and associated variables, while the ARW simulations at the 500-m resolution (i.e., the CSRM simulations) do not use these sub-grid parameterizations based on consideration that the CSRM simulations resolve sub-grid processes. Thus, the CSRM simulations (that prove to act as benchmark simulations through comparisons to observations) are able to evaluate the sub-grid parameterizations in the GFS model. The sub-grid parameterizations are designed to correct errors that are caused by the use of coarse resolutions in the GFS model. However, comparisons between the GFS simulations and the ARW simulations at different resolutions indicate that despite the presence of sub-grid parameterizations in the GFS model, the errors or differences in the updraft intensity and associated cloud variables between the GFS simulations and the CSRM simulations exist due to resolutions. Hence, sub-grid parameterizations need to be improved to better represent sub-grid processes. To this end, results here indicate that sub-grid parameterizations (e.g., scale-aware cumulus schemes) which are being implemented into the NWP models (e.g., the GFS model) should be able to compensate for the over- and under-estimation of weak updrafts and strong updrafts, respectively, due to coarse resolutions.

Comparisons between GFS simulations and ARW simulations also indicate that it is likely that the GFS model underestimates the sensitivity of updrafts and associated cloud variables to increasing aerosol concentrations. In general, parameterizations that represent sub-grid updrafts and other associated variables do not have pathways through which increasing aerosol concentrations affect updrafts and associated cloud variables. However, recent studies by Lim et al. (2014), Thayer-Calder et

Atmos. Chem. Phys. Discuss., https://doi.org/10.5194/acp-2017-501
Manuscript under review for journal Atmos. Chem. Phys.
Discussion started: 6 June 2017

al. (2015), and Griffin and Larson (2016) have attempted to consider interactions among microphysical processes, their variations with varying aerosol concentrations, and sub-grid dynamic (e.g., updrafts and downdrafts) and thermodynamic (e.g., temperature) variables in those parameterizations. These efforts should focus on countering the variation in the sensitivity of updrafts, in particular strong updrafts and thus that of cloud variables, cloud system organization, and precipitation distributions to increasing aerosol concentrations with coarsening resolution. While the pattern of the sensitivity and its variation shown in this study provides valuable information useful for aiding these efforts, results may be different for different cloud types and environments, given the strong dependence of aerosol-cloud interactions on cloud type and environmental conditions. So to aid the efforts in a generalized way, future studies with more cases that involve various types of aerosol-cloud interactions are needed.

582 **Acknowledgements.** This study is supported by NOAA (Grant NOAA-NWS-NWSPO-2015-
583 2004117), which also provided the GFS forecast data.

Atmos. Chem. Phys. Discuss., https://doi.org/10.5194/acp-2017-501
Manuscript under review for journal Atmos. Chem. Phys.
Discussion started: 6 June 2017

608 **References**

609

610 Bogenschutz, P. A., and S. K. Krueger, 2013, A simplified PDF parameterization of subgrid-scale
611 clouds and turbulence for cloud-resolving models, J. Adv. Model. Earth Syst., 5, 195–211,
612 doi:10.1002/jame.20018.
613 Donelan, M. A., B. K. Haus, N. Reul, et al., 2004, On the limiting aerodynamic roughness of the ocean
614 in very strong winds. Geophys. Res. Lett., 31, doi: 10.1029/2004GL019460.
615 Griffin, B. M. and V. E. Larson, 2016, Parameterizing microphysical effects on variances and
616 covariances of moisture and heat content using a multivariate probability density function: a
617 study with CLUBB (tag MVCS), Geosci. Model Dev., 9, 4273-4295, doi:10.5194/gmd-9-4273-
618 2016.
619 Hwang, S.-O., and D.-K. Lee, 1993, A study on the relationship between heavy rainfalls and associated
620 low-level jets in the Korean peninsula, J. Korean Meteorol. Soc., 29, 133–146.
621 Fan J, T. Yuan, J. M. Comstock, et al., 2009. Dominant role by vertical wind shear in regulating aerosol
622 effects on deep convective clouds." J. Geophys. Res., 114, doi:10.1029/2009JD012352.
623 Fan, J., L. R. Leung, Z. Li, H. Morrison, et al., 2012, Aerosol impacts on clouds and precipitation in
624 eastern China: Results from bin and bulk microphysics, J. Geophys. Res., 117, D00K36,
625 doi:10.1029/2011JD016537.
626 Fan, J., L.R. Leung, D. Rosenfeld, Q. Chen, Z. Li, J. Zhang, H. Yan, 2013, Microphysical effect
627 determine macrophysical response for aerosol impact on deep convective clouds, Proceedings of
628 National Academy of Sciences (PNAS), doi:10.1073/pnas.1316830110.
629 Fouquart, Y., and B. Bonnel, B., 1980, Computations of solar heating of the Earth's atmosphere: A new
630 parameterization, Beitr. Phys. Atmos., 53, 35-62.
631 Khain, A. P., D. Rosenfeld, and A. Pokrovsky, 2005, Aerosol impact on the dynamics and microphysics
632 of deep convective clouds, Q. J. R. Meteorol. Soc., 131, 2639–2663, doi:10.1256/qj.04.62.
633 Khain, A., and B. Lynn, 2009, Simulation of a supercell storm in clean and dirty atmosphere using
634 weather research and forecast model with spectral bin microphysics, J. Geophys. Res., 114,
635 D19209, doi:10.1029/2009JD011827.
636 Khain, A. P., et al., 2015, Representation of microphysical processes in cloudresolving models: Spectral
637 (bin) microphysics versus bulk parameterization, Rev. Geophys., 53, 247–322,
638 doi:10.1002/2014RG000468.
639 Kim, J. H., S. S. Yum, S. Shim, et al., 2014, On the submicron aerosol distributions and CCN number
640 concentrations in and around the Korean Peninsula, Atmos. Chem. Phys., 14, 8763-8779,
641 doi:10.5194/acp-14-8763-2014.
642 Lance, S., A. Nenes, C. Mazzoleni, et. al., 2009, Cloud condensation nuclei activity, closure, and
643 droplet growth kinetics of Houston aerosol during the Gulf of Mexico Atmospheric
644 Composition and Climate Study (GoMACCS), J. Geophys. Res., 114, D00F15,
645 doi:10.1029/2008JD011699.
646 Lee, S. S. and G. Feingold, 2013, Aerosol effects on the cloud-field properties of tropical convective

clouds, Atmos. Chem. Phys., 13, 6713-6726.
Lee, S. S., W.-K. Tao, and C. H. Jung, 2014, Aerosol effects on instability, circulations, clouds and precipitation, Advances in Meteorology, Article ID 683950.
Lee, S. S., Z. Li, J. Mok, et al., 2017, Interactions between aerosol absorption, thermodynamics, dynamics, and microphysics and their impacts on a multiple-cloud system, Clim. Dynam., doi: 10.1007/s00382-017-3552-x.
Li, Z., F. Niu, J. Fan, Y. Liu, D. Rosenfeld, and Y. Ding, 2011, Long-term impacts of aerosols on the vertical development of clouds and precipitation, Nature Geo., doi: 10.1038/NGEO1313.
Lim, K. S., J. Fan, L. Y. R. Leung, et al., 2014, Investigation of aerosol indirect effects using a cumulus microphysics parameterization in a regional climate model, J. Geophys. Res., 119, 906-926.
Mlawer, E. J., S. J. Taubman, P. D. Brown, M. J. Iacono, and S. A. Clough, 1997, RRTM, a validated correlated-k model for the longwave, J. Geophys. Res., 102, 16663-16682.
Moorthi, S., H.-L. Pan, and P. Caplan, Changes to the 2001 NCEP operational MRF/AVN global analysis/forecast system, 2001, Technical Procedures Bulletin, 484, 14pp., obtainable at http://www.nws.noaa.gov/om/tpb/484.htm
Morcrette, J.-J., A. Benedetti, A. Ghelli, J.W. Kaiser, A.M. Tompkins, 2011, Aerosol-cloud-radiation interactions and their Impact on ECMWF/MACC forecasts, Technical Memorandum, 660, 35pp.
Morrison, H., and A. Gettelman, 2008: A new two-moment bulk stratiform cloud microphysics scheme in the Community Atmosphere Model, version 3 (CAM3). Part I: Description and numerical tests, J. Climate, 21, 3642--3659, doi10.1175/2008JCLI2105.1.
Morrison, H., G. Thompson, and V. Tatarskii, 2009, Impact of cloud microphysics on the development of trailing stratiform precipitation in a simulated squall line: Comparison of one- and two-moment schemes, Mon. Wea. Rev., 137, 991–1007.
Pan, H.-L., and W.-S. Wu, 1995, Implementing a mass flux convective parameterization package for the NMC Medium-Range Forecast model, NMC Office Note 409, 40 pp.
Randall, D. A., M. E. Schlesinger, V. Galin, V. Meleshko, J.-J. Morcrette, and R. Wetherald, 2006, Cloud Feedbacks. In "Frontiers in the Science of Climate Modeling," J. T. Kiehl and V. Ramanathan, Eds., Cambridge University Press, 217-250.
Seifert, A., and D. Beheng, 2006, A two-moment cloud microphysics parameterization for mixed-phase clouds. Part 2: Maritime vs. continental deep convective storms, Meteorol. Atmos. Phys., 92, 67-82.
Seifert, A., C. Köhler, and K. D. Beheng, Aerosol-cloud-precipitation effects over Germany as simulated by a convective-scale numerical weather prediction model, Atmos. Chem. Phys., 12, 709-725, doi:10.5194/acp-12-709-2012, 2012.
Storer, R.L., S.C. van den Heever, and G.L. Stephens, 2010, Modeling aerosol impacts on convective storms in different environments, J. Atmos. Sci., 67, 3904-3915.
Sudhakar, D., J. Quaas, R. Wolke, J. Stoll, A. Mühlbauer, M. Salzmann, B. Heinold, and I. Tegen, 2016, Implementation of aerosol-cloud interactions in the regional atmosphere-aerosol model COSMO-MUSCAT and evaluation using satellite data, Geosci. Model Dev. Discuss., doi:10.5194/gmd-2016-186.

687 Sun, J., T.-Y. Lee, 2002, A numerical study of an intense quasistationary convection band over the
688 Korean peninsula, J. Meteorol. Soc. Jpn., 80, 1221–1245.
689 Sundqvist, H., E. Berge, and J. E. Kristjansson, 1989, Condensation and cloud parameterization studies
690 with a mesoscale numerical weather prediction model, Mon. Weather Rev., 117, 1641-1657.
691 Tao, W.-K., X. Li, A. Khain, T. Matsui, S. Lang, and J. Simpson, 2007, The role of atmospheric aerosol
692 concentration on deep convective precipitation: cloud-resolving model simulations, J. Geophys.
693 Res., 112, D24S18, doi:10.1029/2007JD008728.
694 Tao, W.-K., J. P. Chen, Z. Li, and C. Zhang, 2012, Impact of aerosols on convective clouds and
695 precipitation, Rev. of Geophy., 50, RG2001, doi:10.1029/2011RG000369.
696 Thayer-Calder, K., A. Gettelman, C. Craig, et al., 2015, A unified parameterization of clouds and
697 turbulence using CLUBB and subcolumns in the Community Atmosphere Model, Geosci.
698 Model Dev., 8, 3801-3821, doi:10.5194/gmd-8-3801-2015.
699 van den Heever, S.C., and W.R. Cotton, 2007, Urban aerosol impacts on downwind convective storms,
700 J. Appl. Meteor. Climatol., 46, 828-850.
701 van den Heever, S. C., G. L. Stephens, and N. B. Wood, 2011, Aerosol indirect effects on tropical
702 convection characteristics under conditions of radiative-convective equilibrium, J. Atmos. Sci.,
703 68, 699-718.
704 Wang, H., W. C. Skamarock, and G. Feingold, 2009, Evaluation of scalar advection schemes in the
705 Advanced Research WRF model using large-eddy simulations of aerosol-cloud interactions,
706 Mon. Wea. Rev., 137, 2547-2558.
707 Zeng, X., and A. Beljaars, 2005, A prognostic scheme of sea surface skin temperature for modeling and
708 data assimilation, Geophys. Res. Lett, 32, L14605, doi:10.1029/2005GL023030, 2005.
709 Zhao, Q. Y., and F. H. Carr, 1997, A prognostic cloud scheme for operational NWP models, Mon. Wea.
710 Rev., 125, 1931- 1953.
711

712

713

714

715

716

717

718

Atmos. Chem. Phys. Discuss., https://doi.org/10.5194/acp-2017-501
Manuscript under review for journal Atmos. Chem. Phys.
Discussion started: 6 June 2017

719 **Tables**

720

721 Table 1. Description of the simulations.

Simulations	Case	Aerosol number concentration at the surface (cm^{-3})	Microphysics scheme	Resolution	Saturation	Sedimentation	Collection
High-aerosol-Seoul run	Seoul	5500	Bin	500 m	Supersaturation prediction	Bin-scheme sedimentation	Bin-scheme collection
Low-aerosol-Seoul run	Seoul	550	Bin	500 m	Supersaturation prediction	Bin-scheme sedimentation	Bin-scheme collection
High-aerosol-Houston run	Houston	1500	Bin	500 m	Supersaturation prediction	Bin-scheme sedimentation	Bin-scheme collection
Low-aerosol-Houston run	Houston	150	Bin	500 m	Supersaturation prediction	Bin-scheme sedimentation	Bin-scheme collection
High-aerosol-15-Seoul run	Seoul	5500	Bin	15 km	Supersaturation prediction	Bin-scheme sedimentation	Bin-scheme collection
Low-aerosol-15-Seoul run	Seoul	550	Bin	15 km	Supersaturation prediction	Bin-scheme sedimentation	Bin-scheme collection
High-aerosol-15-Houston run	Houston	1500	Bin	15 km	Supersaturation prediction	Bin-scheme sedimentation	Bin-scheme collection
Low-aerosol-15-Houston	Houston	150	Bin	15 km	Supersaturation prediction	Bin-scheme sedimentation	Bin-scheme collection

Atmos. Chem. Phys. Discuss., https://doi.org/10.5194/acp-2017-501
Manuscript under review for journal Atmos. Chem. Phys.
Discussion started: 6 June 2017

run							
High-areosol-35-Seoul run	Seoul	5500	Bin	35 km	Supersaturation prediction	Bin-scheme sedimentation	Bin-scheme collection
Low-aerosol-35-Seoul run	Seoul	550	Bin	35 km	Supersaturation prediction	Bin-scheme sedimentation	Bin-scheme collection
High-aerosol-35-Houston run	Houston	1500	Bin	35 km	Supersaturation prediction	Bin-scheme sedimentation	Bin-scheme collection
Low-aerosol-35-Houston run	Houston	150	Bin	35 km	Supersaturation prediction	MG-scheme sedimentation	MG-scheme collection
High-aerosol-MG-Seoul run	Seoul	5500	MG	500 m	Saturation adjustment	MG-scheme sedimentation	MG-scheme collection
Low-aerosol-MG-Seoul run	Seoul	550	MG	500 m	Saturation adjustment	MG-scheme sedimentation	MG-scheme collection
High-aerosol-MG-Houston run	Houston	1500	MG	500 m	Saturation adjustment	MG-scheme sedimentation	MG-scheme collection
Low-aerosol-MG-Houston run	Houston	150	MG	500 m	Saturation adjustment	MG-scheme sedimentation	MG-scheme collection
High-aerosol-sat-Seoul run	Seoul	5500	Bin	500 m	Saturation adjustment	Bin-scheme sedimentation	Bin-scheme collection
Low-aerosol-sat-Seoul run	Seoul	550	Bin	500 m	Saturation adjustment	Bin-scheme sedimentation	Bin-scheme collection
High-aerosol-	Houston	1500	Bin	500 m	Saturation	Bin-scheme	Bin-scheme

Atmos. Chem. Phys. Discuss., https://doi.org/10.5194/acp-2017-501
Manuscript under review for journal Atmos. Chem. Phys.
Discussion started: 6 June 2017

sat-Houston run					adjustment	sedimentation	collection
Low-aerosol-sat-Houston run	Houston	150	Bin	500 m	Saturation adjustment	Bin-scheme sedimentation	Bin-scheme collection
High-aerosol-sed-Seoul run	Seoul	5500	Bin	500 m	Saturation adjustment	MG-scheme sedimentation	Bin-scheme collection
Low-aerosol-sed-Seoul run	Seoul	550	Bin	500 m	Saturation adjustment	MG-scheme sedimentation	Bin-scheme collection
High-aerosol-sed-Houston run	Houston	1500	Bin	500 m	Saturation adjustment	MG-scheme sedimentation	Bin-scheme collection
Low-aerosol-sed-Houston run	Houston	150	Bin	500 m	Saturation adjustment	MG-scheme sedimentation	Bin-scheme collection
High-aerosol-col-Seoul run	Seoul	5500	Bin	500 m	Saturation adjustment	MG-scheme sedimentation	MG-scheme collection
Low-aerosol-col-Seoul run	Seoul	550	Bin	500 m	Saturation adjustment	MG-scheme sedimentation	MG-scheme collection
High-aerosol-col-Houston run	Houston	1500	Bin	500 m	Saturation adjustment	MG-scheme sedimentation	MG-scheme collection
Low-aerosol-col-Houston run	Houston	150	Bin	500 m	Saturation adjustment	MG-scheme sedimentation	MG-scheme collection

722

Atmos. Chem. Phys. Discuss., https://doi.org/10.5194/acp-2017-501
Manuscript under review for journal Atmos. Chem. Phys.
Discussion started: 6 June 2017

FIGURE CAPTIONS

Figure 1. (a) Sea-level pressure (hPa) and (b) 850 hPa wind (m s^{-1}; arrows), geopotential height (m; contours) and equivalent potential temperature (K; shaded) at 0900 LST July 26th 2011 over the northeast Asia. The rectangles in the Korean Peninsula in panels (a) and (b) mark the center of Seoul. (c) Sea-level pressure (hPa;shaded) and wind at 10 m above sea level (m s^{-1}; barbs) and (d) convective available potential energy (J kg^{-1}) at 0500 LST 18 July 2013 in and around Houston. The rectangles in panels (c) and (d) mark the center of Houston.

Figure 2. (a) The domain (marked by the rectangle) used in simulations for the Seoul case. The small white circle marks the center of Seoul. (b) The domain used in simulations for the Houston case. The small white circle marks the center of Houston.

Figure 3. Vertical distributions of the time- and domain-averaged cloud liquid content (CLC) for (a) the Seoul case and (b) the Houston case. Solid lines represent simulations at the 500-m resolution, while dashed lines represent those at the 15-km resolution. Dotted lines represent simulations at the 35-km resolution and blue lines represent GFS-simulated CLC.

Figure 4. Same as Figure 3, but for cloud ice content (CIC).

Atmos. Chem. Phys. Discuss., https://doi.org/10.5194/acp-2017-501
Manuscript under review for journal Atmos. Chem. Phys.
Discussion started: 6 June 2017

744 Figure 5. Time series of the domain-averaged (a) liquid water path (LWP) and (b) ice water path
745 (IWP) for the Seoul case. Solid lines represent simulations at the 500-m resolution, while dashed and
746 dotted lines represent those at 15-km and 35-km resolutions, respectively. Blue lines represent GFS-
747 simulated LWP and IWP and green lines represent observed LWP and IWP.
748
749 Figure 6. Same as Figure 5, but for the Houston case.
750
751 Figure 7. Vertical distributions of the time- and domain-averaged updraft mass fluxes for (a) the Seoul
752 case and (b) the Houston case. Solid lines represent simulations at the 500-m resolution, while dashed
753 lines represent those at the 15-km resolution. Dotted lines represent simulations at the 35-km resolution
754 and blue lines represent GFS-simulated updraft mass fluxes.
755
756 Figure 8. Vertical distributions of the time- and domain-averaged condensation rates for (a) the Seoul
757 case and (b) the Houston case. Solid lines represent simulations at the 500-m resolution, while dashed
758 lines represent those at the 15-km resolution. Dotted lines represent simulations at the 35-km resolution.
759
760 Figure 9. Same as Figure 8, but for deposition rates.
761

762 Figure 10. Distributions of normalized updraft frequency over updraft speeds for (a) the Seoul case
763 and (b) the Houston case. Solid lines represent simulations at the 500-m resolution, while dashed lines
764 represent those at the 15-km resolution. Dotted lines represent simulations at the 35-km resolution.
765
766 Figure 11. Same as Figure 8, but for evaporation rates.
767
768 Figure 12. Distributions of normalized precipitation frequency over precipitation rates for (a) the Seoul
769 case and (b) the Houston case. Solid lines represent simulations at the 500-m resolution, while dashed
770 lines represent those at the 15-km resolution. Dotted lines represent simulations at the 35-km resolution.
771
772 Figure 13. Vertical distributions of the time- and domain-averaged cloud liquid content (CLC) for (a)
773 the Seoul case and (b) the Houston case. Solid red and black lines represent simulations with the bin
774 scheme and at the 500-m resolution, while dashed red and black lines represent the bin-scheme
775 simulations with the saturation adjustment. Solid yellow and green lines represent simulations with the
776 MG scheme.
777
778 Figure 14. Vertical distributions of the time- and domain-averaged cloud liquid content (CLC) for (a)
779 the Seoul case and (b) the Houston case. Solid red and black lines represent simulations with the bin
780 scheme and at the 500-m resolution, while dashed red and black lines represent the bin-scheme

Atmos. Chem. Phys. Discuss., https://doi.org/10.5194/acp-2017-501
Manuscript under review for journal Atmos. Chem. Phys.
Discussion started: 6 June 2017

simulations with the saturation adjustment and the MG scheme sedimentation process. Solid yellow and green lines represent simulations with the MG scheme.

Figure 15. Vertical distributions of the time- and domain-averaged cloud liquid content (CLC) for (a) the Seoul case and (b) the Houston case. Solid red and black lines represent simulations with the bin scheme and at the 500-m resolution, while dashed red and black lines represent the bin-scheme simulations with the saturation adjustment and the MG scheme sedimentation and collection processes. Solid yellow and green lines represent simulations with the MG scheme.

Atmos. Chem. Phys. Discuss., https://doi.org/10.5194/acp-2017-501
Manuscript under review for journal Atmos. Chem. Phys.
Discussion started: 6 June 2017

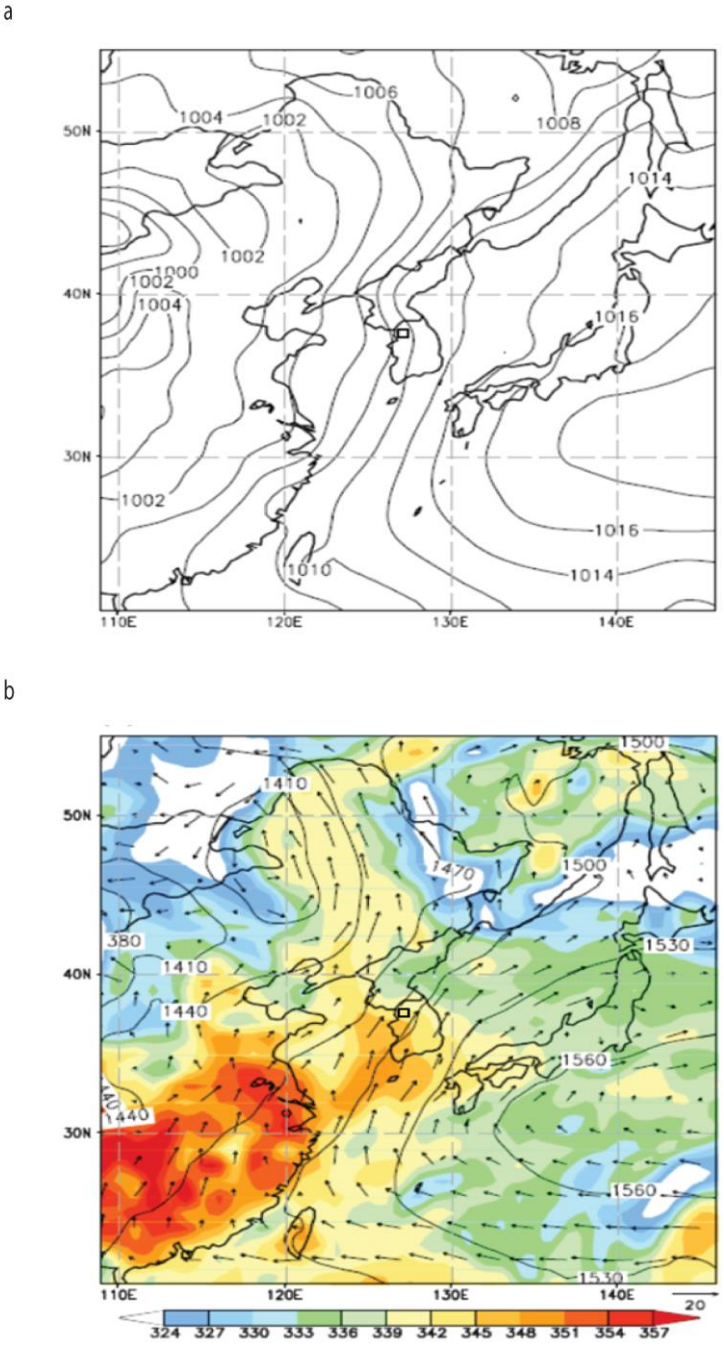

Figure 1

Atmos. Chem. Phys. Discuss., https://doi.org/10.5194/acp-2017-501
Manuscript under review for journal Atmos. Chem. Phys.
Discussion started: 6 June 2017

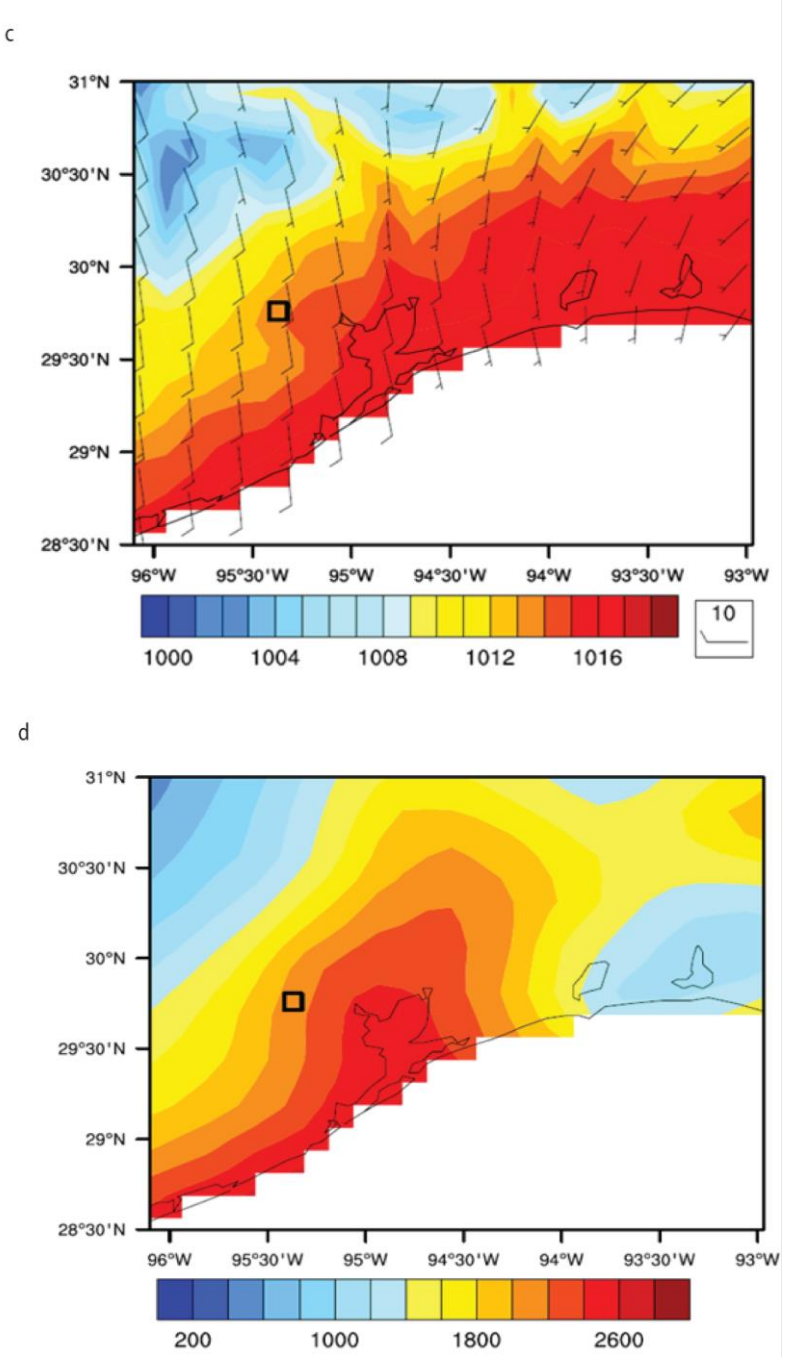

Figure 1

Atmos. Chem. Phys. Discuss., https://doi.org/10.5194/acp-2017-501
Manuscript under review for journal Atmos. Chem. Phys.
Discussion started: 6 June 2017

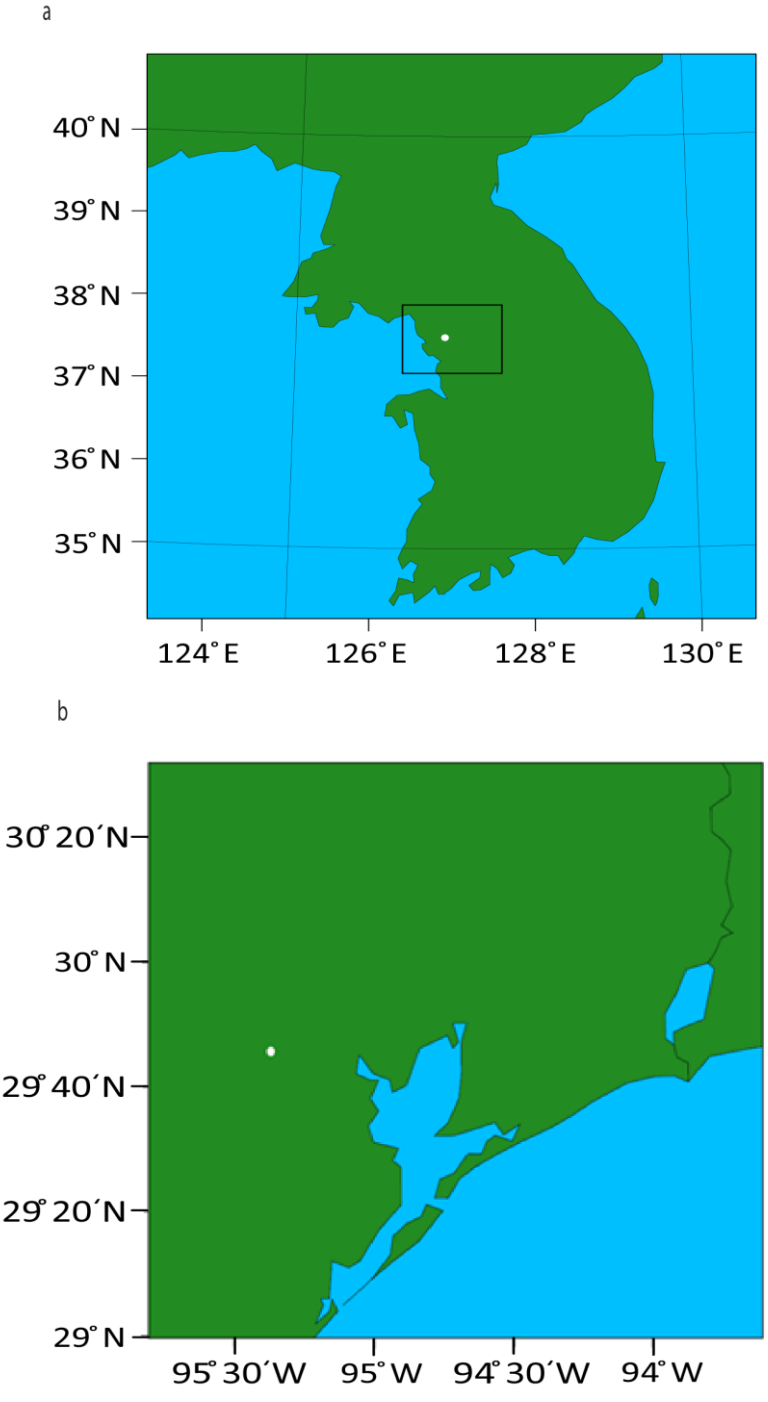

Figure 2

Atmos. Chem. Phys. Discuss., https://doi.org/10.5194/acp-2017-501
Manuscript under review for journal Atmos. Chem. Phys.
Discussion started: 6 June 2017

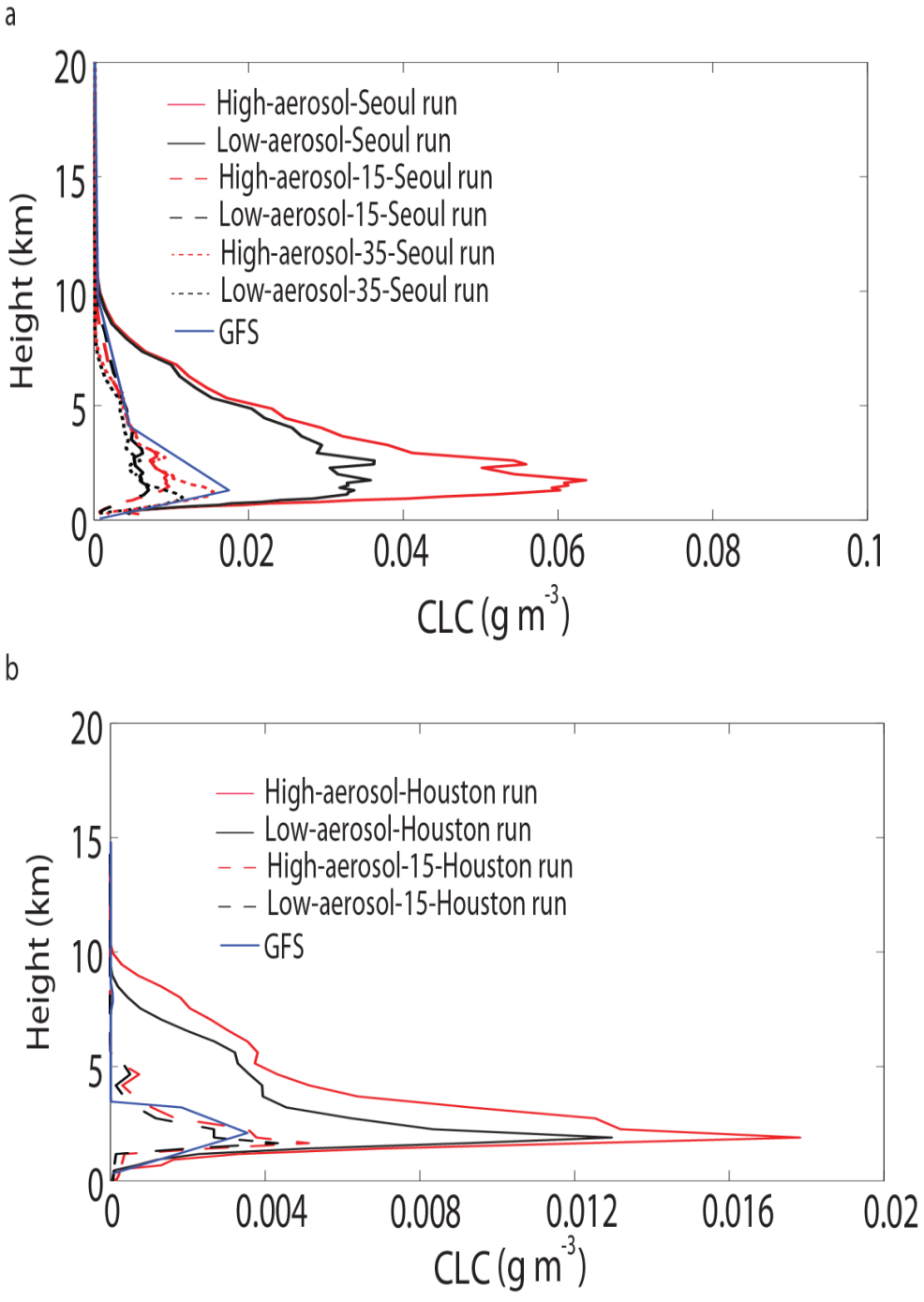

807

808 **Figure 3**

Atmos. Chem. Phys. Discuss., https://doi.org/10.5194/acp-2017-501
Manuscript under review for journal Atmos. Chem. Phys.
Discussion started: 6 June 2017

Atmospheric Chemistry and Physics Discussions

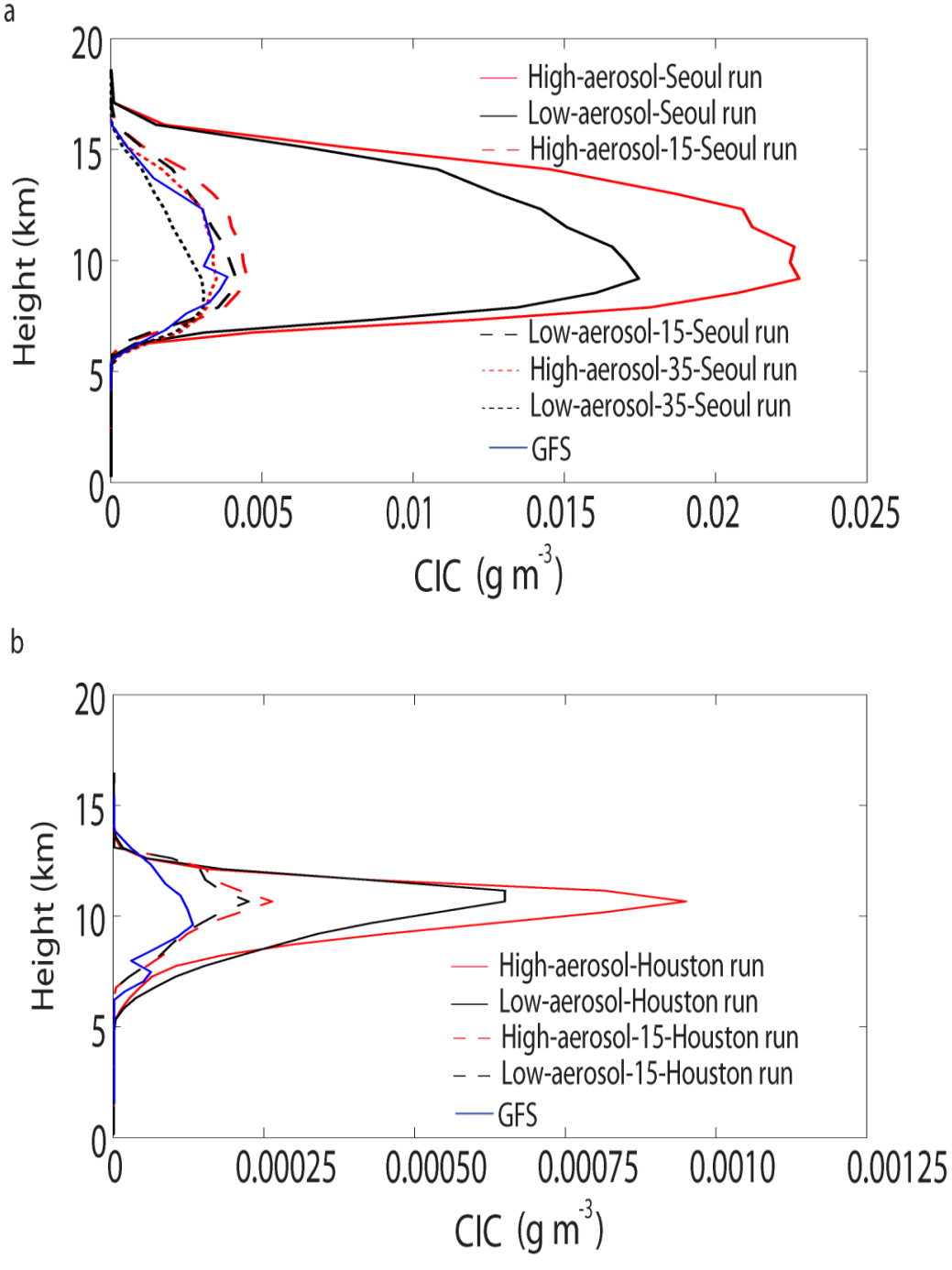

Figure 4

Atmos. Chem. Phys. Discuss., https://doi.org/10.5194/acp-2017-501
Manuscript under review for journal Atmos. Chem. Phys.
Discussion started: 6 June 2017

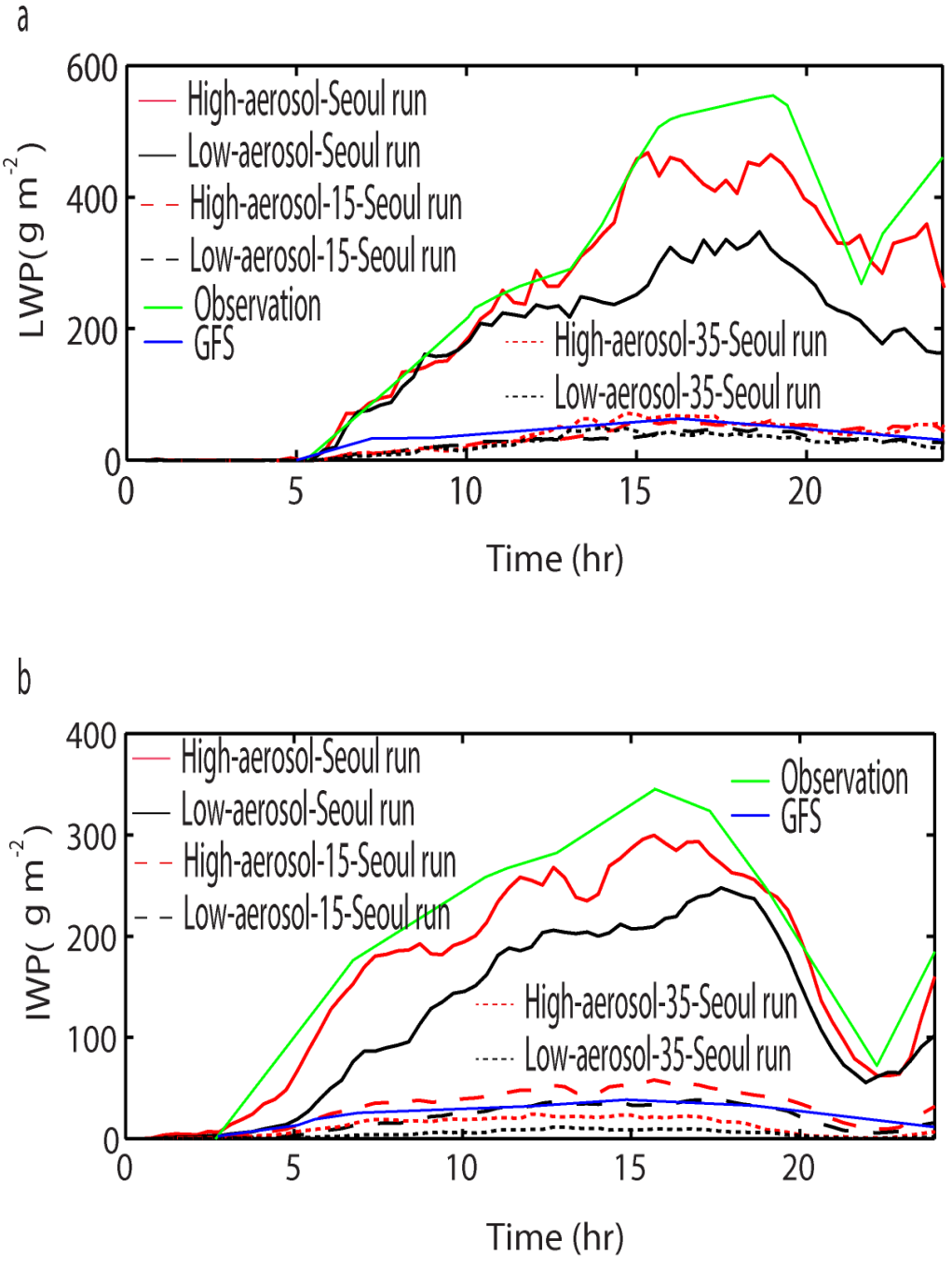

Figure 5

Atmos. Chem. Phys. Discuss., https://doi.org/10.5194/acp-2017-501
Manuscript under review for journal Atmos. Chem. Phys.
Discussion started: 6 June 2017

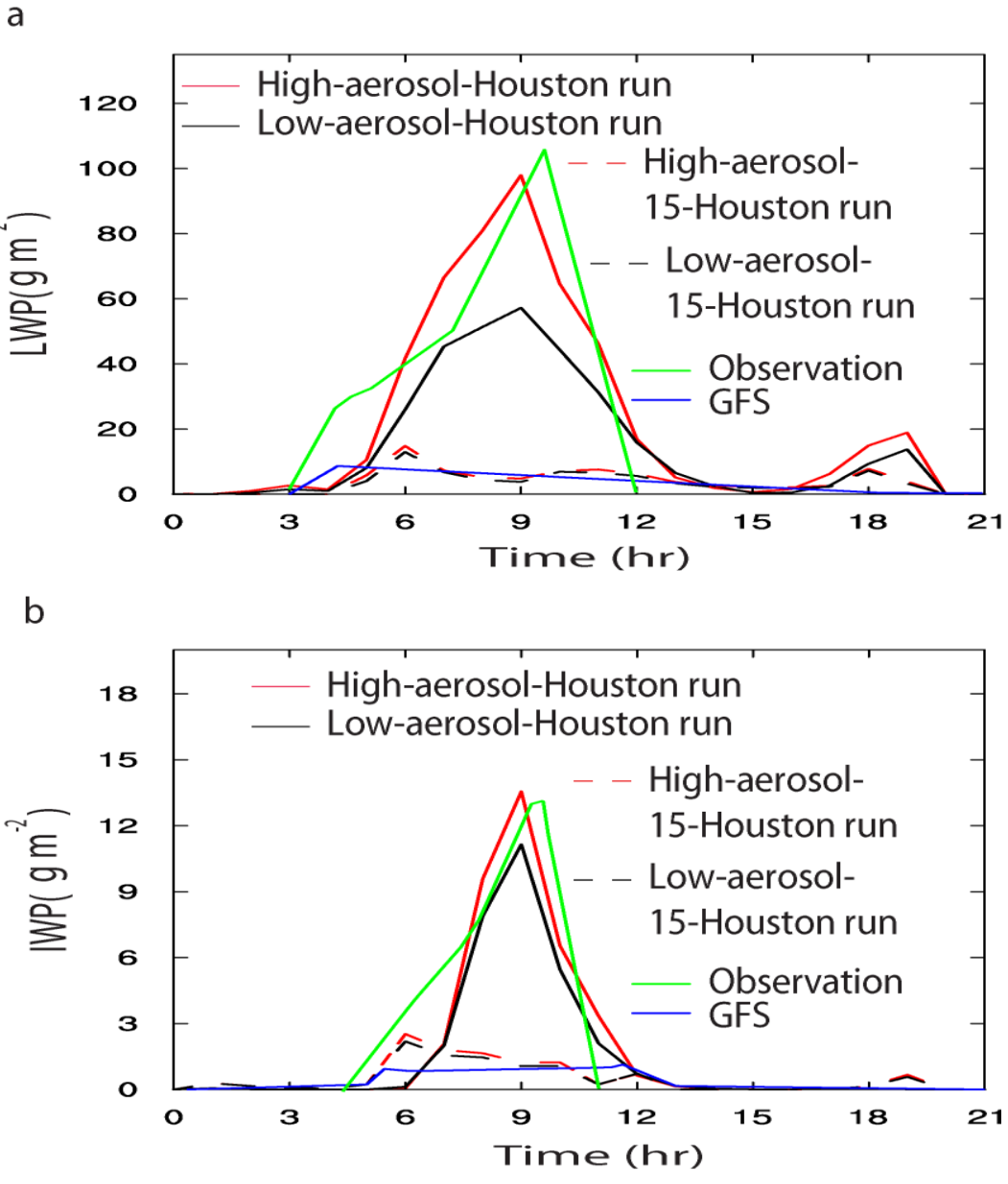

Figure 6

Atmos. Chem. Phys. Discuss., https://doi.org/10.5194/acp-2017-501
Manuscript under review for journal Atmos. Chem. Phys.
Discussion started: 6 June 2017

a

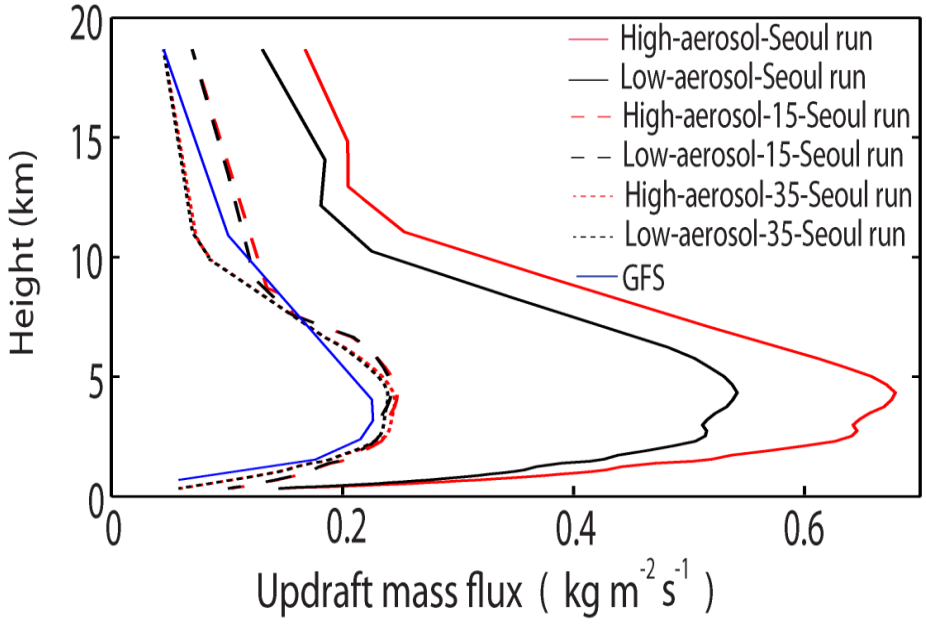

b

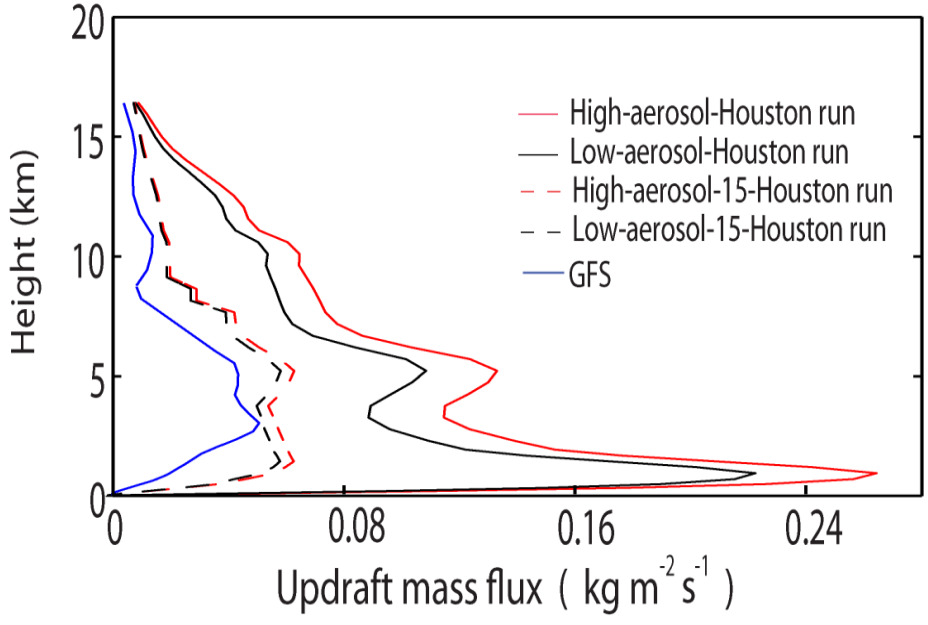

Figure 7

Atmos. Chem. Phys. Discuss., https://doi.org/10.5194/acp-2017-501
Manuscript under review for journal Atmos. Chem. Phys.
Discussion started: 6 June 2017

a

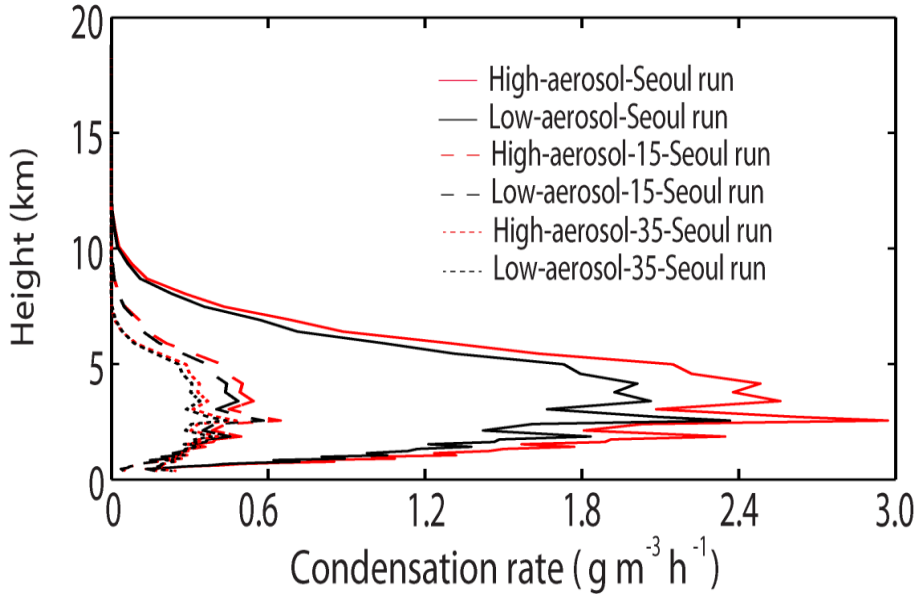

b

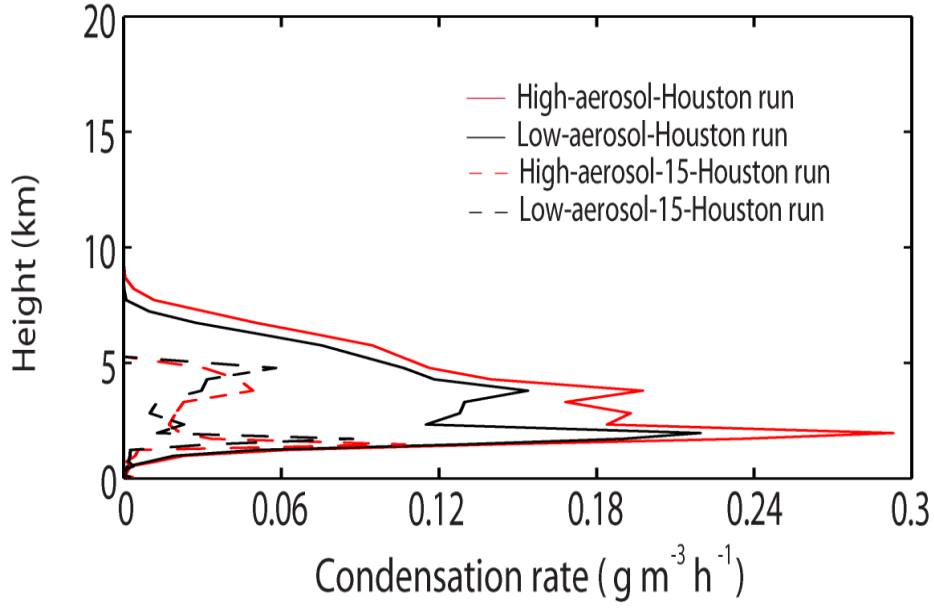

817

818 **Figure 8**

Atmos. Chem. Phys. Discuss., https://doi.org/10.5194/acp-2017-501
Manuscript under review for journal Atmos. Chem. Phys.
Discussion started: 6 June 2017

Atmospheric Chemistry and Physics Discussions

50

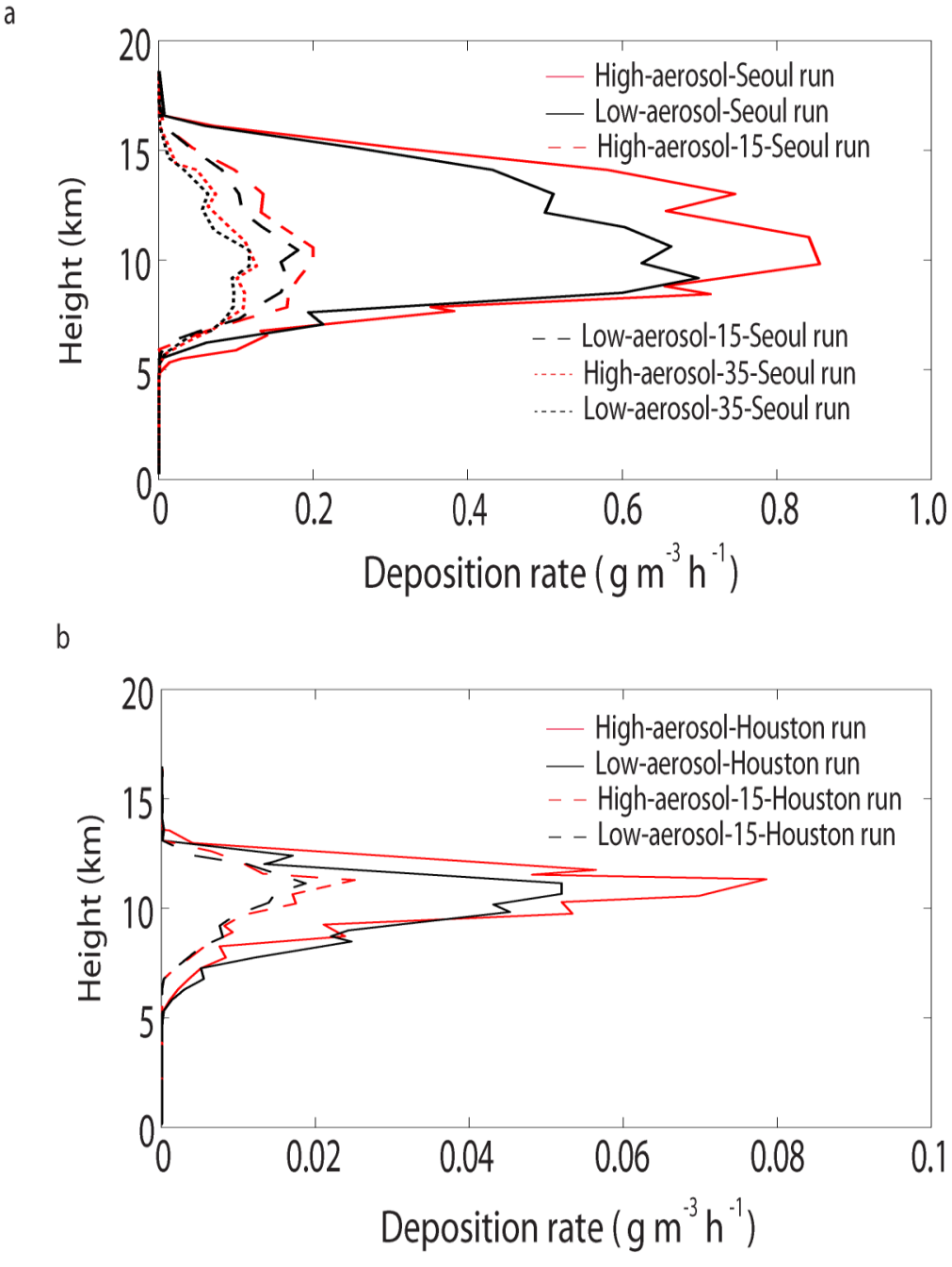

819

820 **Figure 9**

Atmos. Chem. Phys. Discuss., https://doi.org/10.5194/acp-2017-501
Manuscript under review for journal Atmos. Chem. Phys.
Discussion started: 6 June 2017

a

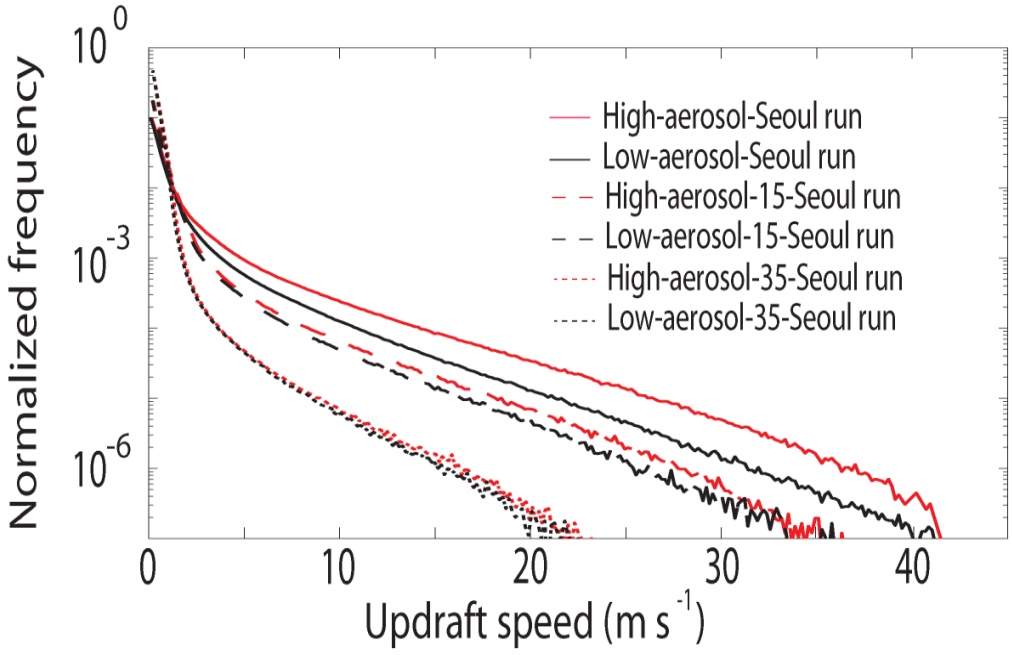

b

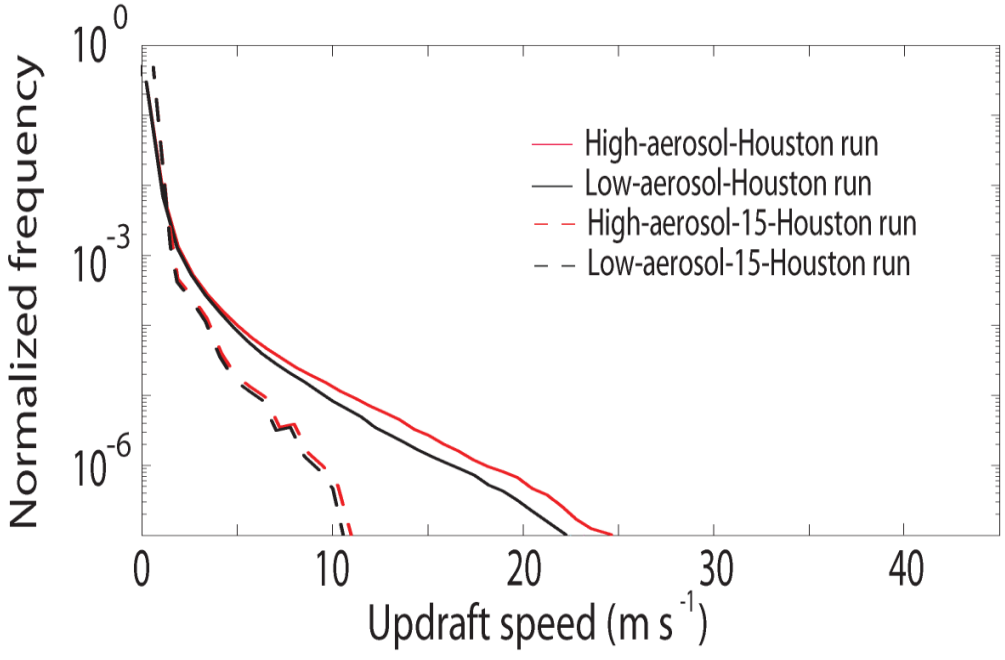

821

822 **Figure 10**

Atmos. Chem. Phys. Discuss., https://doi.org/10.5194/acp-2017-501
Manuscript under review for journal Atmos. Chem. Phys.
Discussion started: 6 June 2017

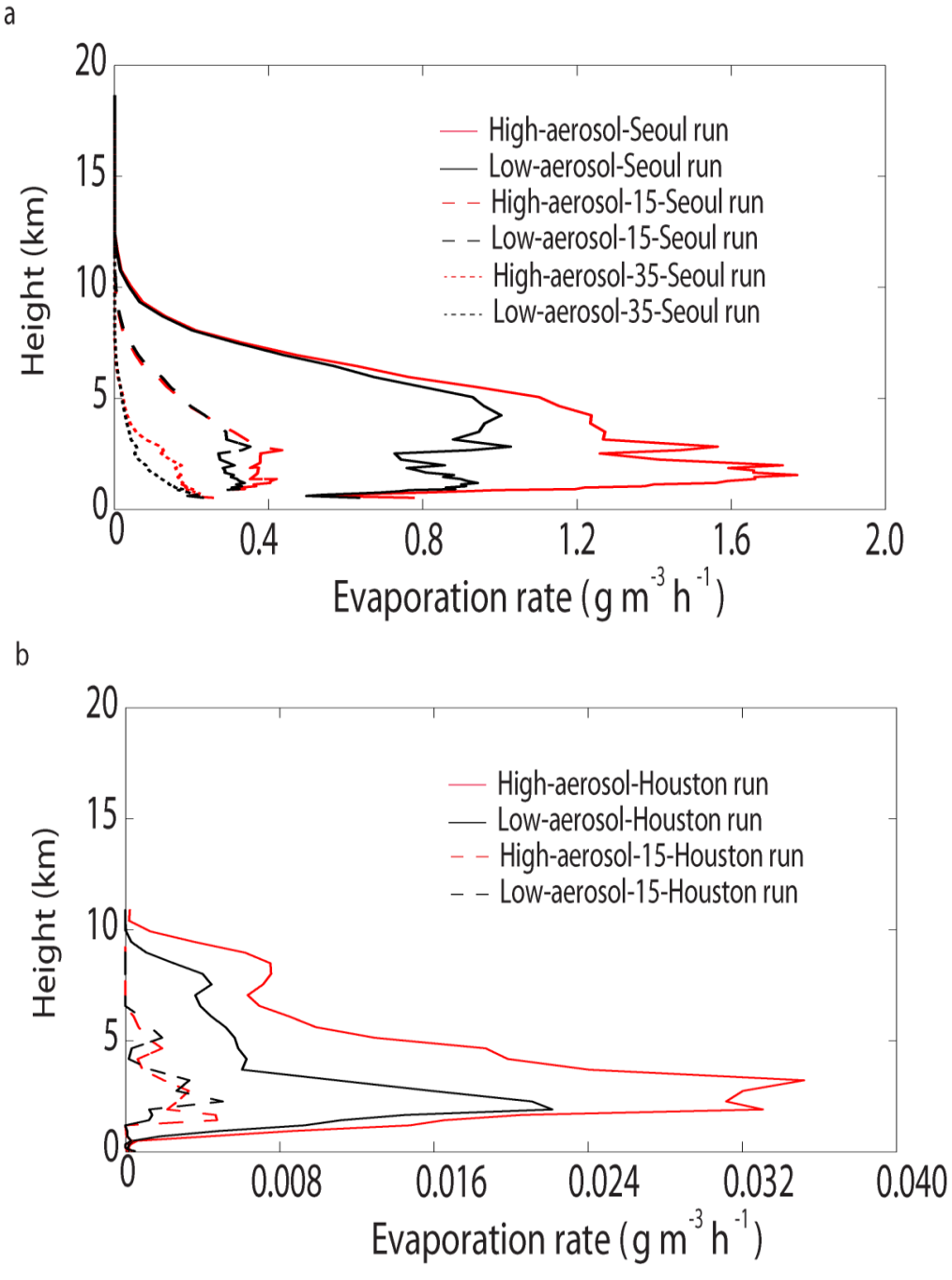

Figure 11

Atmos. Chem. Phys. Discuss., https://doi.org/10.5194/acp-2017-501
Manuscript under review for journal Atmos. Chem. Phys.
Discussion started: 6 June 2017

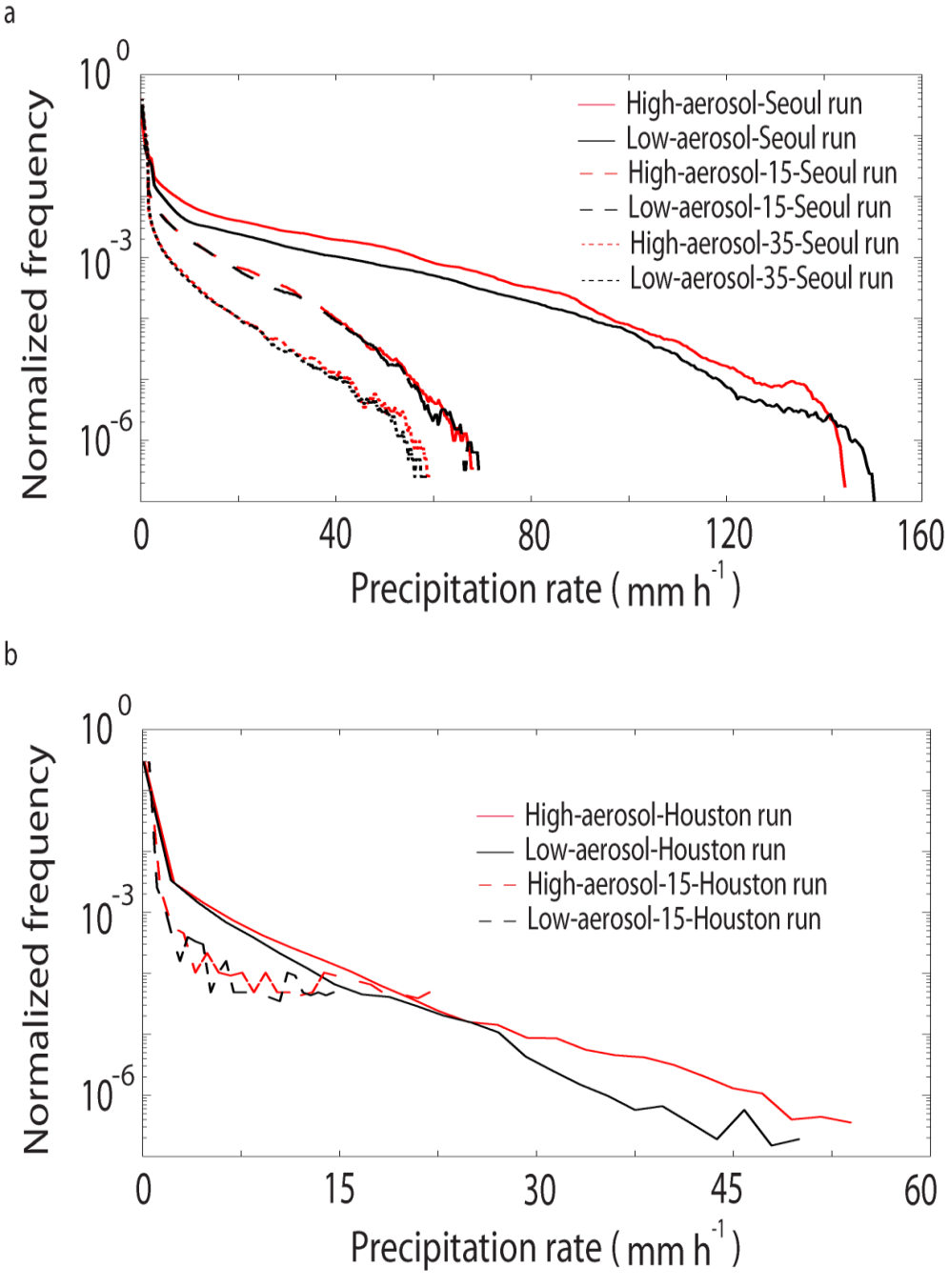

Figure 12

Atmos. Chem. Phys. Discuss., https://doi.org/10.5194/acp-2017-501
Manuscript under review for journal Atmos. Chem. Phys.
Discussion started: 6 June 2017

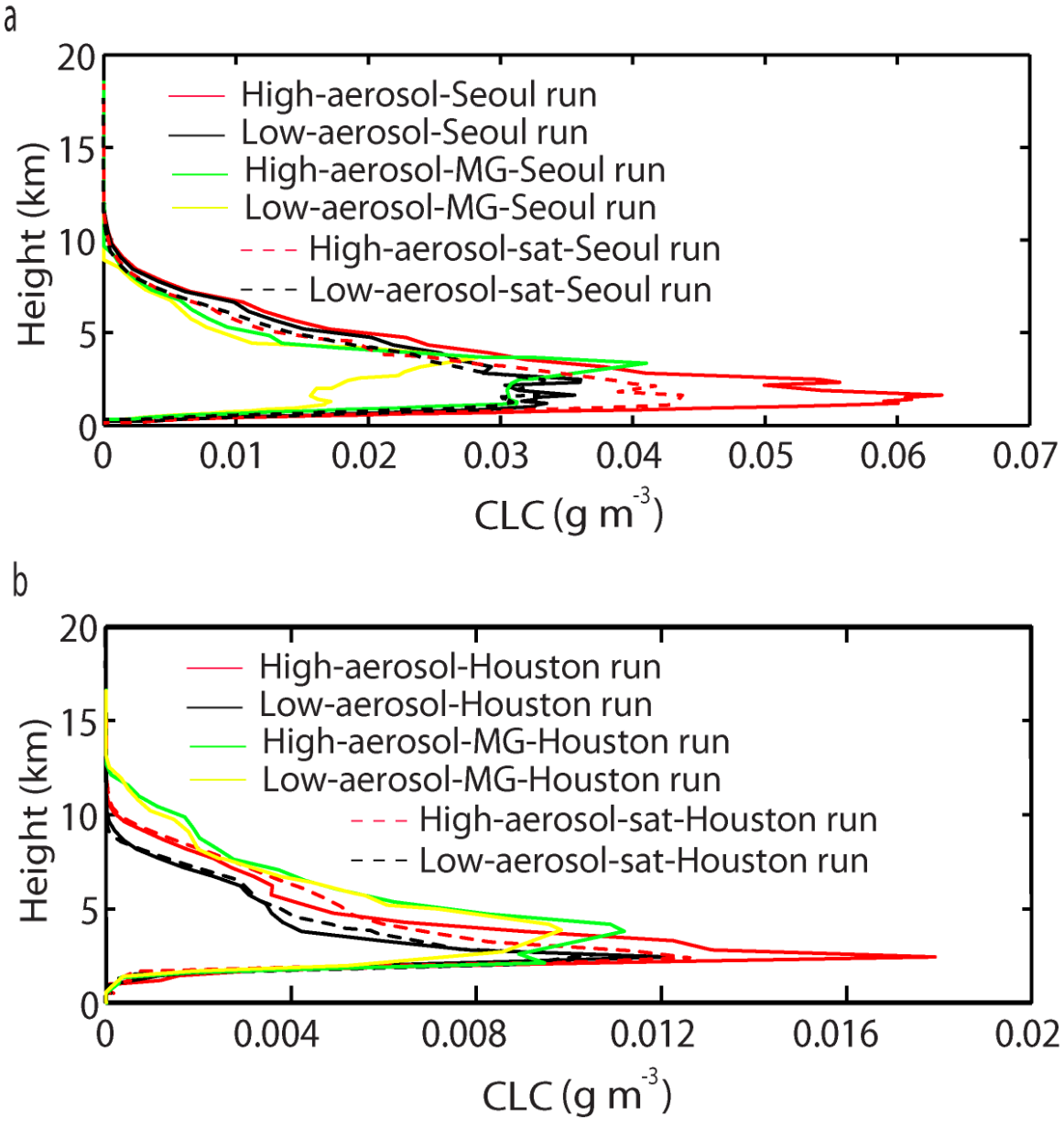

827

828 **Figure 13**

829

Atmos. Chem. Phys. Discuss., https://doi.org/10.5194/acp-2017-501
Manuscript under review for journal Atmos. Chem. Phys.
Discussion started: 6 June 2017

Atmospheric Chemistry and Physics Discussions

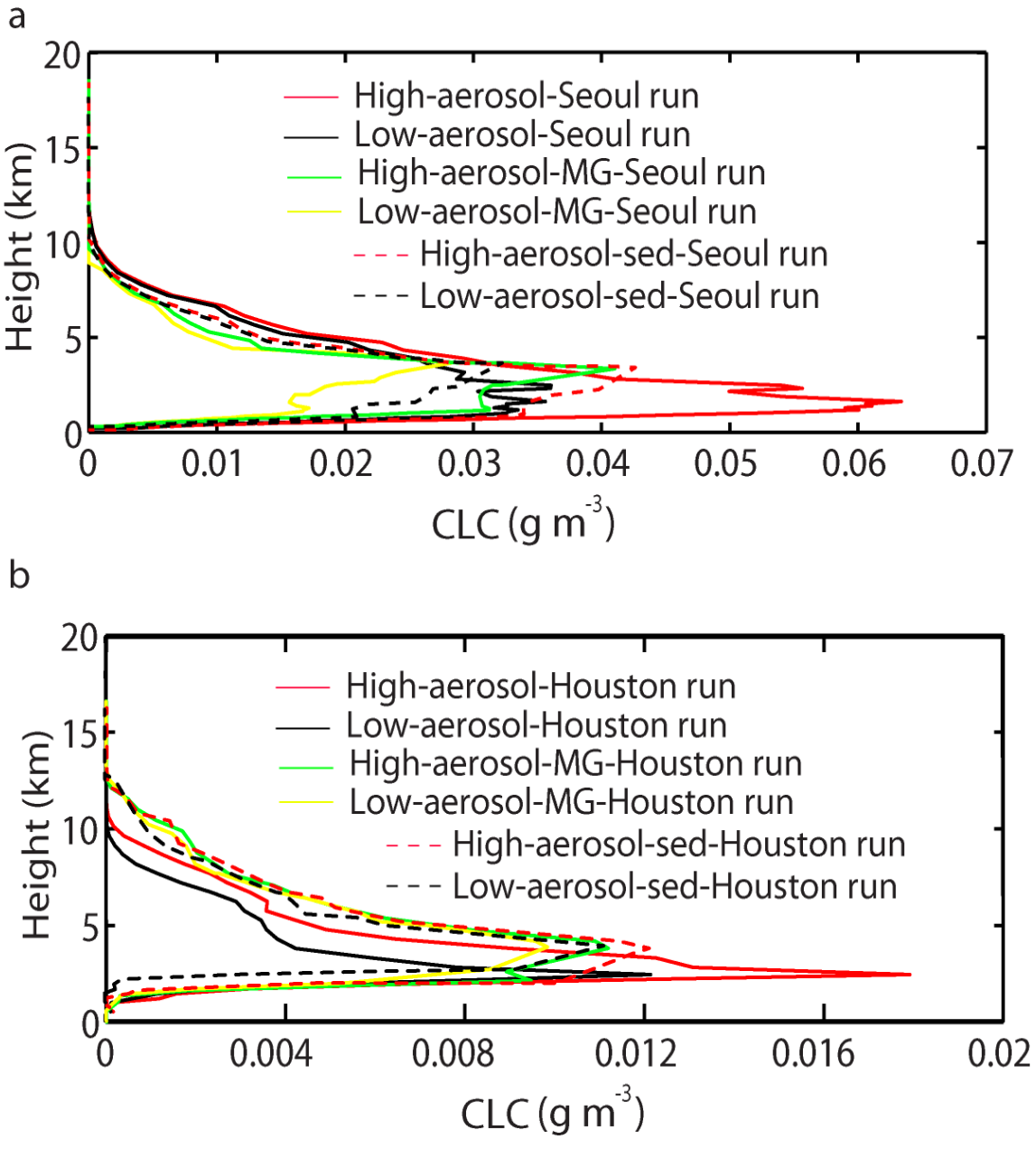

Figure 14

Atmos. Chem. Phys. Discuss., https://doi.org/10.5194/acp-2017-501
Manuscript under review for journal Atmos. Chem. Phys.
Discussion started: 6 June 2017

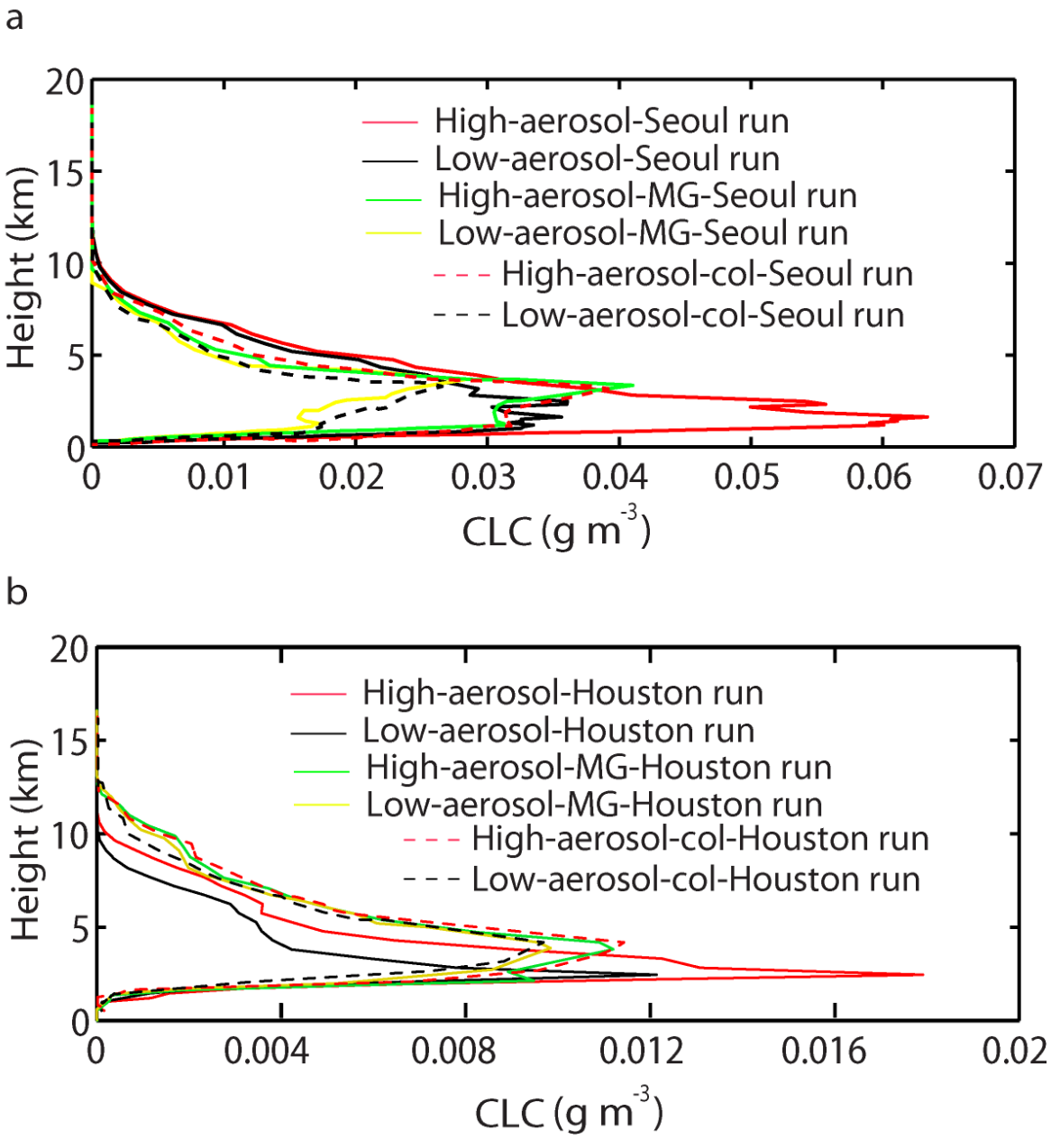

Figure 15